SANDIA REPORT

SAND2017-5472
Unlimited Release
Printed May 2017

Fault Analysis and Detection in Microgrids with High PV Penetration

Mohamed E. Elkhatib, Javier Hernandez-Alvidrez and Abraham Ellis

Prepared by
Sandia National Laboratories
Albuquerque, New Mexico 87185 and Livermore, California 94550

Sandia National Laboratories is a multi-mission laboratory managed and operated by Sandia Corporation, a wholly owned subsidiary of Lockheed Martin Corporation, for the U.S. Department of Energy's National Nuclear Security Administration under contract DE-AC04-94AL85000.

Issued by Sandia National Laboratories, operated for the United States Department of Energy by Sandia Corporation.

Available to DOE and DOE contractors from
U.S. Department of Energy
Office of Scientific and Technical Information
P.O. Box 62
Oak Ridge, TN 37831

Telephone: (865) 576-8401
Facsimile: (865) 576-5728
E-Mail: reports@adonis.osti.gov
Online ordering: http://www.osti.gov/bridge

Available to the public from
U.S. Department of Commerce
National Technical Information Service
5285 Port Royal Rd
Springfield, VA 22161

Telephone: (800) 553-6847
Facsimile: (703) 605-6900
E-Mail: orders@ntis.fedworld.gov
Online ordering: http://www.ntis.gov/help/ordermethods.asp?loc=7-4-0#online

SAND2017-5472
Unlimited Release
Printed May 2017

Fault Analysis and Detection in Microgrids with High PV Penetration

Mohamed E. Elkhatib, Javier Hernandez-Alvidrez and Abraham Ellis
Electric Power Systems Research
Sandia National Laboratories
MS 1140, P.O. Box 5800
Albuquerque, NM 87185-1140
email: meelkha@sandia.gov

Abstract

keywords: Microgrids, Protection Analysis, PV Inverters, Fault Analysis

In this report we focus on analyzing current-controlled PV inverters behaviour under faults in order to develop fault detection schemes for microgrids with high PV penetration. Inverter model suitable for steady state fault studies is presented and the impact of PV inverters on two protection elements is analyzed. The studied protection elements are superimposed quantities based directional element and negative sequence directional element. Additionally, several non-overcurrent fault detection schemes are discussed in this report for microgrids with high PV penetration. A detailed time-domain simulation study is presented to assess the performance of the presented fault detection schemes under different microgrid modes of operation.

Contents

List of Figures

1 Introduction

Development of efficient non-overcurrent based protection schemes is a prerequisite for significantly increasing microgrids renewable energy penetration. The main challenge facing the development of standardized microgrid protection originates from the fact that microgrids differ in their topology, generation mix, feeder sizes and fault interruption devices types and locations. Additionally, fault current levels could change drastically between grid-connected and islanded modes of operation which makes it very difficult, or even impossible in some cases, to maintain overcurrent protection coordination for both cases. Moreover, in the islanded mode of operation, fault currents could change significantly with generation dispatch which complicates protection coordination design. Further, for microgrids with significant inverter-interfaced generation, renewable generation for example, fault currents could be very limited as a result of inverter current-limiting control functions which typically limit fault contribution to as low as 1.1 per unit. Therefore, overcurrent protection could fail completely to pick up the fault in the first place.

Typically, distribution-connected PV inverters operate in current-control mode which means that the inverter continuously control it's terminal voltage in order to maintain the output current at a certain target level. During faults, the terminal voltage and current of PV inverters will be primarily governed by their controllers and thus the relation between the output voltage and current will generally be nonlinear. In contrast, during faults, a conventional synchronous machine typically behave as a constant voltage source behind an impedance. It is important to notice that most protection scheme designs in literature, such as directional elements, were developed assuming synchronous machines-based sources. Therefore, there is a need to investigate the performance of different protection elements under high penetration of current-controlled PV inverters.

Additionally, since fault current contribution of PV inverters is small, there is a need to develop non-overcurrent protection schemes for microgrids with high inverter-based resources. Several microgrid non-overcurrent protection schemes were introduced in literature. A voltage based protection schemes was discussed in [1]. The method is based on the fact that during faults, voltage levels dips across the microgrid. However, discriminating between faults and other normal-operation events based on voltage levels, such as capacitor tripping, is hard to achieve. Additionally, in a typical microgrid, the magnitude of voltage dip during faults would be the same in different locations due to small feeder lengths; therefore, determining fault location based on voltage magnitude could be very difficult. Reference [2] used voltage-based protection in combination with directional elements to develop protection scheme for low fault low voltage radial microgrids. Communication-assisted voltage-based protection for radial medium-voltage microgrids was proposed in [3].
A differential protection scheme for low-fault microgrids was proposed in [4]. That scheme is based on installing fault interrupting devices and differential relays at both ends of each feeder segment of the microgrid. Additionally, the scheme requires communication channel for each protection zone and it rely on synchronized measurement of currents at both ends of each line segment. That scheme could clearly provide a robust protection solution for low-fault microgrids in both modes of operation. However, the cost of such scheme could

be prohibitively high given two breakers must be installed at both ends of each microgrid feeder segment. Therefore, unless the particular application of a microgrid justify the cost, it is hard to see that scheme used widely for typical microgrids. A differential-based sequence component protection scheme was proposed in [5] which assumes protection zone granularity similar to [4] but it requires more processing time and more extensive communication infrastructure without any improvement in protection robustness. The application of traditional distance protection for microgrids, and generally for distribution systems, was discussed in [6]. However, distance protection is not typically efficient when applied to tapped feeders since it will cause the relay to underreach and thus complicates coordination between different relays.
Several protection methods based on transient behaviour of faults was discussed in literature. In [7], a travelling wave based protection scheme was presented. The scheme is based on measuring timing and polarity of the initial waves at both side of the protected line after the occurrence of the fault. It is not clear what is the triggering event which the relays will use to start measuring the incident wave travelling time. Additionally, for a typical microgrid it is very hard to discriminate between incident waves travelling timing to different locations due to the relatively small feeders lengths compared with travelling waves speed. Moreover, the method require protection zone granularity similar to differential protection proposed in [4], however, differential protection is way more robust. Protection schemes based on wavelet analysis of fault currents was presented in [8] and [9]. These papers only discussed faults at the terminals of DGs and there is no discussion about how the scheme will detect feeder faults midway between DGs. Additionally, as for other transient based methods, there is no general proof that the transient signature used in the proposed protection is universal and does not depend on the microgrid configuration or generation dispatch.
A communication-assisted impedance-based protection scheme was proposed as part of this research project [10]. The proposed scheme depends on monitoring impedance trajectories at different feeder relays to detect the occurrence of faults and utilizes directional elements to determine the direction of faults. Communications between feeder relays are utilized to exchange permissive and blocking signals in order to locate the fault and trip the least part of the microgrid to clear the fault.

This report starts with a detailed analysis of PV current-controlled inverters behaviour under faults. The objective is to analyze inverter's impact on protection elements design and fault analysis in microgrids with high PV penetration. Based on that analysis, inverter model suitable for steady state fault studies is presented and the impact of PV inverters on two protection elements is analyzed. The studied protection elements are superimposed quantities based directional element and negative sequence directional element. Additionally, several non-overcurrent fault detection schemes are discussed in this report for microgrids with high PV penetration. A detailed time-domain simulation study is presented to assess the performance of the presented fault detection schemes under different microgrid modes of operation.

2 Analysis of PV Inverters under faults

In this section the performance of PV current-controlled inverters under balanced and unbalanced faults is reviewed. The goal is to analyze inverter characteristics pertaining to protection systems design. Fig.9 shows the control structure of a typical distribution-connected current-controlled PV inverters. It basically consists of two main control loops: an inner current control loop and an outer power control loop. The current control loop is responsible for regulating the output current of the inverter, i_d and i_q, while the power control loop is responsible for adjusting the reference current of the current controllers, i_{dqref}. Typically, direct current component reference, i_{dref}, is determined by the Maximum Power Point Tracking (MPPT) controller of the PV. Meanwhile, quadrature component of the reference current, i_{qref}, is determined based on the reactive power control strategy of the PV inverter and could also be controlled to enhance the LVRT capability of the PV inverter.

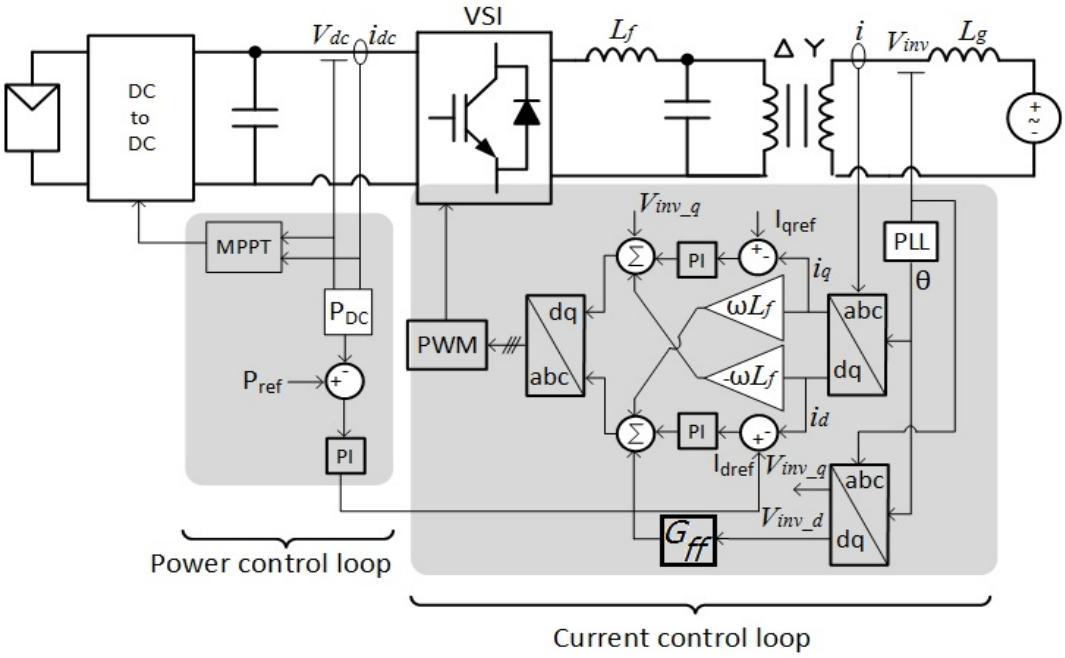

Figure 1: Control structure of PV inverters used for this study

2.1 Balanced Faults

The occurrence of a balanced fault in the microgrid will result in a drop in the magnitude and change in the phase of the grid voltage at the terminals of the inverter. The response of the inverter to the fault can be divided into three temporal stages. In the first stage, due to the drop in grid voltage V_{sdq}, the output current i_{dq} will start to increase. Also, since V_{sdq} experienced sudden phase shift, the PLL will lose synchronization with the grid and will start to change its output phase to re-synchronous with the new phase of the grid voltage. As a results, the output current i_{dq} might experience transients in magnitude and phase. Practically though, this stage will be very brief since inverter's current controller is typically

fast to regain phase lock and regulate the output current. Therefore, for protection design purposes, this stage is typically ignored.

In the second stage, the current control loop will start regulating the output current, i_{dq}, to maintain their values at the respective i_{dqref} which corresponds to the pre-fault output current. The response of the inverter in the second stage depends on the design of the current PI controller. Typically, current controllers are designed with fast dynamics to quickly regulate inverter's output current.

The drop of the grid voltage combined with the current controller's actions to maintain inverter's output current at the pre-fault level, results in a drop in the output power of the inverter. Such a drop in inverters output power will cause inverter's DC voltage to increase which in turn will increase the i_{dref} as shown in Fig.9. Additionally, based on the reactive power operation strategy of the PV inverter, i_{qref} will also change to recover the reactive power output of the inverter. Thus in the third stage, the output current of the inverter will change in response to the change in the reference current i_{dref}. Typically, output current will increase to maintain the output active and reactive power of the inverter fixed under depressed grid voltage. The dynamics of the third stage is slower than that of the second stage but is typically fast relative to the microgrid's protection functions.

Therefore, after the PLL locks to the new grid voltage under fault and the output power recovers to the pre-fault levels, the phase angle between the output current and the new grid voltage in the post-fault case will be similar to the phase angle between the output current and the grid voltage under the pre-fault case.

In the case of a close in fault particularly if the pre-fault power output was relatively high, the output current of the inverter could increase, based on the above analysis, beyond a certain manufacturer-specific limit. In such case, the inverter would typically enter a constant current control mode and the output current will be limited to protect the power electronics switches regardless of the output power level. The current limit of PV inverters varies but is typically in the range of 1.1 to 1.4 pu.

In conclusion, for protection design purposes, the inverter will act as a current limited constant power source under balanced faults as shown in Fig.2. It is important to notice that depending on the pre-fault power output of the PV and the location of the fault, the short circuit current contribution of the inverter could actually be even less than 1 pu based on Fig.2. As a result, detecting faults in microgrids with high penetration of PV could be very challenging.

2.2 Unbalanced Faults

The operation of current-controlled voltage source inverters under unbalanced faults has been studied extensively in literature. In this section we will highlight the important aspects of inverter behaviour under unbalanced faults which pertain to microgrid protection system design. Under unbalanced faults, the grid voltage at the terminals of the inverter will gen-

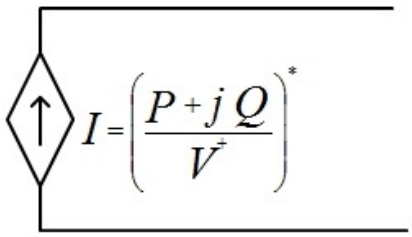

Figure 2: Equivalent circuit of PV inverters under balanced faults

erally contain positive, negative and zero sequence components. Typical PV inverters are connected to the grid through a grounded-Wye/delta transformers, therefore, the inverter will not generate nor be impacted by the zero sequence component of the grid voltage. On the other hand, negative sequence component of the grid voltage can have an impact on the inverter operation. Assuming the PLL is under steady state conditions, the dq components of the grid voltage can be expressed as [11]:

$$V_{sd} = V_1 + V_2 cos(2\omega_0 t + 2\theta_0) \tag{1}$$

$$V_{sq} = -V_2 sin(2\omega_0 t + 2\theta_0) \tag{2}$$

Generally, PV PLLs are designed to filter out the 120Hz ripple of the V_{sq}. Thus we will assume that the PLL is synchronized with the positive sequence component and that its outputs, ω_0 and θ_0, are ripple-free.

Additionally, the voltage feedforward scheme shown in Fig.9 will essentially *add* the 120Hz components of the grid voltage shown in equations (1) and (2) to the inverter's output voltage. Thus, inverter's output voltage will, theoretically, have a negative sequence component that equals and is opposed to the negative sequence component of the grid voltage. As a result, the inverter output current will, more or less, be balanced and distortion-free. However, it is important to notice that in practice the ability of the PV inverter to keep the output current balanced under unbalanced grid voltage depends on design factors including inverter's switching frequency and the ability of the feedforward scheme to faithfully reproduce the 120Hz component of the grid voltage, which depends on the bandwidth of the feedforward compensator G_{ff}. These factors varies from manufacturer to another and thus the degree of distortion and amount of unbalance in inverter's output current will depend to some extend on the specific case under study. For protection related studies, we will assume in the following analysis that PV inverters output current are balanced and distortion-free under unbalanced grid voltage.

As the power output of the PV inverter decreases during the fault, the outer power loop will change the reference currents i_{dqref} to compensate for the reduction in power as discussed in section 2.1. Assuming the PLL is synchronized with the positive sequence component of the grid voltage, inverter's active power can be written as:

$$P_{out} = \frac{3}{2} i_d V_{sd} \tag{3}$$

$$Q_{out} = -\frac{3}{2} i_q V_{sd} \tag{4}$$

substituting of equation (1) in equations (3) and (4) results in:

$$P_{out} = \frac{3}{2} i_d V_1 + \frac{3}{2} i_d V_2 cos(2\omega_0 t + 2\theta_0) \tag{5}$$

$$Q_{out} = -\frac{3}{2} i_q V_1 + \frac{3}{2} i_q V_2 cos(2\omega_0 t + 2\theta_0) \tag{6}$$

Assuming that inverter's output current is balanced as discussed earlier, i_d and i_q will be more or less DC values. Thus, equations (5) and (6) indicate that the output powers of the inverter will have 120Hz components with zero average. The 120Hz component in the active power will result in the creation of 120Hz ripple on the DC voltage. Ideally, the outer power loop will change i_{dqref} to maintain constant power outputs. For example based on (5) and (6), i_{dref} can be calculated to maintain constant output power as follows:

$$i_{dref} = \frac{2}{3} \frac{P_{out}}{V_1 + V_2 cos(2\omega_0 t + 2\theta_0)} \tag{7}$$

$$i_{qref} = -\frac{2}{3} \frac{Q_{out}}{V_1 + V_2 cos(2\omega_0 t + 2\theta_0)} \tag{8}$$

However, since the current control loop is designed to handle DC signals under normal operation and due to the typically large size of he interface inductance L, typically i_{dq} output of the inverter will not change much in response to the 120Hz ripple in the power loop. Thus for dq-controlled PV inverter, the output current will, to a large extend, be affected by the average of the output power expressed in equations (4) and (5). In other words, on average,

$$i_d = \frac{2}{3} \frac{P_{out}}{V_1} \tag{9}$$

$$i_q = -\frac{2}{3} \frac{Q_{out}}{V_1} \tag{10}$$

which means that the inverter will increase its current output to ensure that the positive sequence power is fixed. Clearly, there are other control strategies studied in the literature which control the inverter under unbalanced faults for different objectives such as minimizing or removing the pulsation in the output power, thus removing the DC side ripples, see [12, 13, 14, 15, 16, 17] for details on these strategies. However, currently, in typical commercial PV dq-controlled inverters, these strategies tend not to be implemented.

In conclusion, under unbalanced faults, typical dq-controlled PV inverter will inject mostly positive sequence current although a small negative sequence current could also be injected by the inverter depending on the inverter's controller characteristics. The injected current

will be controlled to ensure that the output positive sequence power equals to the pre-fault power output of the inverter. Additionally, the phase angle between inverter's output current and the positive sequence component of the grid voltage in the post-fault case will be similar to the pre-fault case. Finally, the inverter would typically exhibit 120Hz ripple in the DC voltage the magnitude of which depends on the amount of unbalance in the grid voltage.

2.3 Inverter Model for Fault Studies

Based on the analysis presented in sections 2.1 and 2.2, a PV inverter could be modelled, in the ideal case, in short circuit studies as shown in Fig.3 where the inverter is represented by a constant current source in the positive sequence circuit and open circuits for the negative and zero sequence circuits. Therefore, PV inverters would typically prevent negative and zero sequence currents but could have negative sequence voltage at their terminals.

On the other hand, Fig.4 shows the conventional short circuit model of synchronous machines where the machine is represented by a constant voltage source in the positive sequence network and short circuit in the negative and zero sequence networks. Thus negative and zero sequence currents could flow through the synchronous machine but negative sequence voltages would not appear on the terminals of the machine. Additionally, synchronous machines tend to maintain the phase angle of their internal voltage post fault, at least initially. However, for inverters, the phase angle of the output current is shifted based on the post-fault terminal voltage which is determined by the grid.

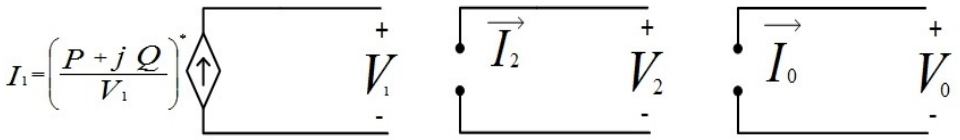

Figure 3: Equivalent ideal sequence network for PV inverters

2.4 Impact of High PV Penetration on Protection Elements Operation

As discussed in sections 2.1 and 2.2, the behaviour of current-controlled inverters under faults is fundamentally different from that of conventional synchronous machines. Therefore, there is a need to study the performance of conventional protection elements under high penetration of PV inverters. In this section, the impact of high inverter penetration on the performance of two protection elements is investigated.

2.4.1 Negative sequence-based directional elements

Negative sequence directional elements has been applied successfully for years in practice. Broadly speaking, two types of negative sequence-based directional elements are used widely:

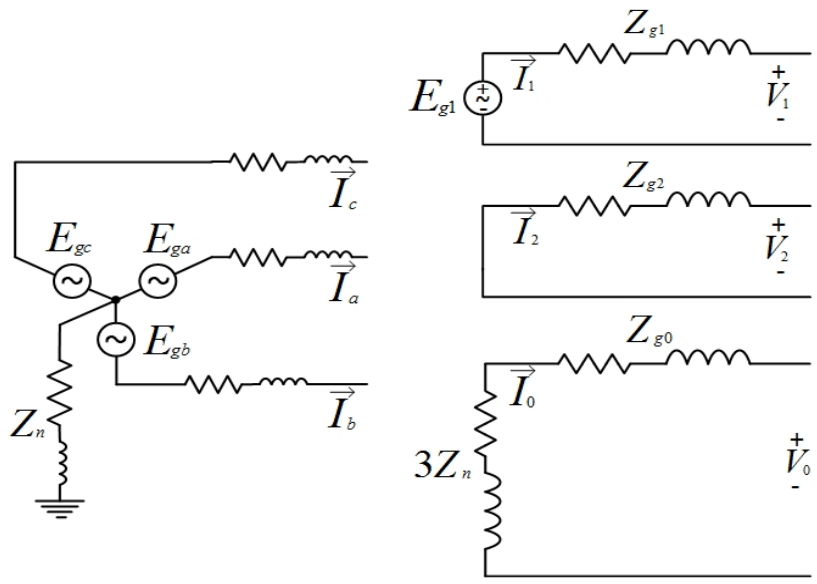

Figure 4: Equivalent sequence network for conventional synchronous generators

traditional negative-sequence directional element and negative-sequence impedance directional element [18].

Generally, negative sequence directional elements is based on measuring the phase difference between the negative sequence voltage measured at the relay terminals and the negative sequence current flowing through relay point. However, it should be noted that the underlying design principles of negative sequence-based elements are driven based on the sequence components equivalent circuit of synchronous machines.

To clarify this concept, consider the system of Fig.5. Since synchronous machines are represented by a short circuit in the negative sequence network, the negative sequence current seen by the relay is completely determined by the negative sequence network. Thus, a negative sequence impedance directional element could be designed to measure the negative sequence impedance as follows [18]:

$$Z_{2-meas} = \frac{Re[V_2.(1\angle Z_{line}.I_2)^*]}{|I_2|^2} \tag{11}$$

where, for forward faults, Z_{2-meas} will be equal to $-Z_s$ and for reverse fault, Z_{2-meas} will equal to $Z_G + Z_l$.

On the other hand, consider Fig.6 where the synchronous machine used in Fig.5 is replaced by a current-controlled PV inverter. In this case, the negative sequence current will be governed by the inverter controller. Typically, as discussed in section 2.2, the inverter will inject balanced current which means, ideally, the negative sequence current will be zero and the negative sequence-based directional element should be deactivated. However, in reality, a small negative sequence current could be flowing at the inverter terminals. While the magnitude of such current will typically be small, the angle of that current is governed by

the inverter dynamics and will be hard to predict under all system conditions. As a result, a negative sequence directional element might not function properly under high penetration of PV inverters.

It is also important to notice that while the *microgrid equivalent* was represented in Fig.6 with an equivalent synchronous machine, this assumption might not even be true for microgrids with high PV penetration. In fact, depending on the penetration of PV inverters, there might be a need to have a more detailed microgrid "equivalent" model to account for the impact of inverters on the overall negative sequence current flow.

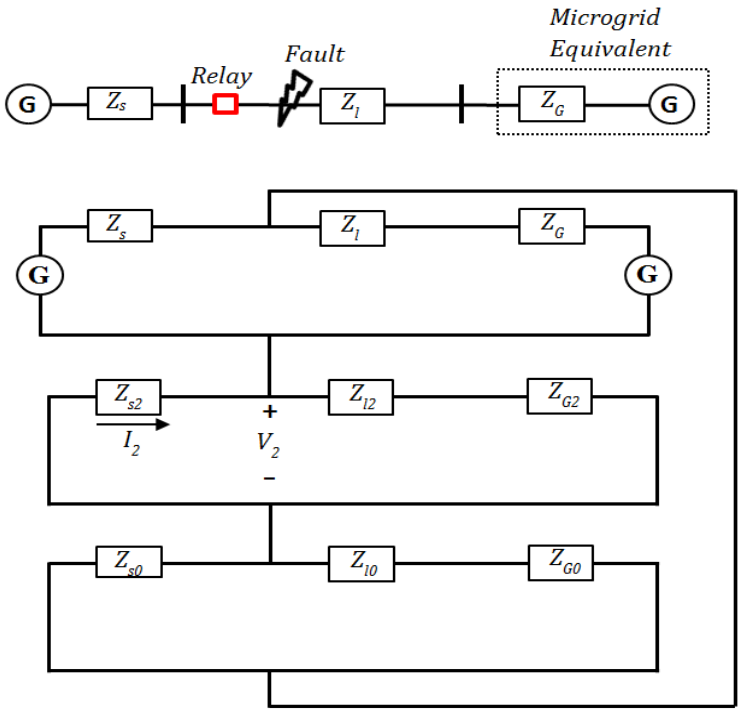

Figure 5: Equivalent sequence network with synchronous generator for a forward fault

2.4.2 Superimposed quantities-based elements

By comparing post fault quantities to pre fault quantities, it is possible to calculate incremental voltages and currents which are exclusively driven by the fault. These quantities are called superimposed and they enable the analysis of pure fault circuits [19]. Superimposed quantities-based protection elements have the advantage of been immune to the impact of normal load. Traditionally, in order to create pure-fault circuit for superimposed quantities analysis, all sources are suppressed and a voltage source is applied at the fault location. This assumption is based on the the fact that, during faults, synchronous machines could be represented as an ideal constant voltage source behind an impedance. Fig.7 shows an example of creating a pure-fault equivalent circuit. The incremental impedance at the relay could be defined as follows:

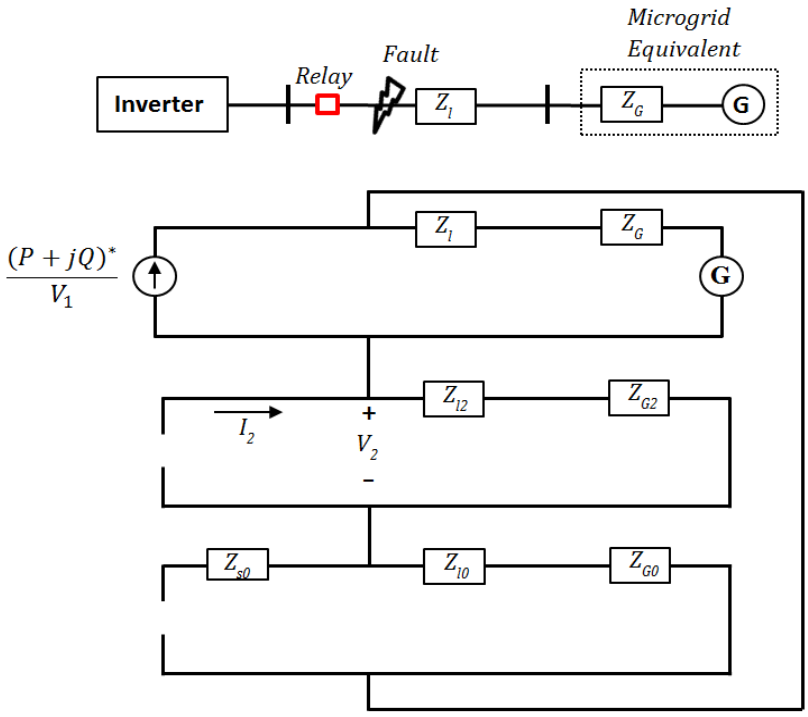

Figure 6: Equivalent sequence network with PV inverter for a forward fault

$$\Delta Z = \frac{\Delta V}{\Delta I} \tag{12}$$

Based on Fig.7, ΔZ will equal to negative Z_s which means a forward fault. Thus, a simple directional element could be designed based on the resulting sign of ΔZ as follows [20]: if sign of ΔZ is negative, the fault direction is forward and if sign of ΔZ is positive, the fault direction is reverse. Additionally, more secure directional elements, and various distance elements, could be designed based on monitoring the locus of ΔZ in the $R - X$ plane, see [20],[21],[22] for example.

However, current-controlled PV inverters do not act as constant voltage sources behind impedance during fault but rather experience fast changes in terminal voltages based on their control strategy. Therefore, using the above described procedure to create *pure-fault* equivalent circuits and analyze superimposed quantities for microgrids with high PV penetration is not accurate. As a matter of fact, one could argue that, since the behaviour of PV inverters during faults is nonlinear, it is not possible to create pure fault equivalent circuit with high penetration of PV.

Theoretically speaking, a current-controlled inverter could be represented as a constant voltage source behind a variable impedance. The variable impedance is necessary to match the, potentially highly nonlinear, $V - I$ relation at the terminals of the inverter during the fault. Consequently, the above mentioned superimposed directional relay based on the sign of the incremental impedance, as calculated by 12, might function properly under high PV

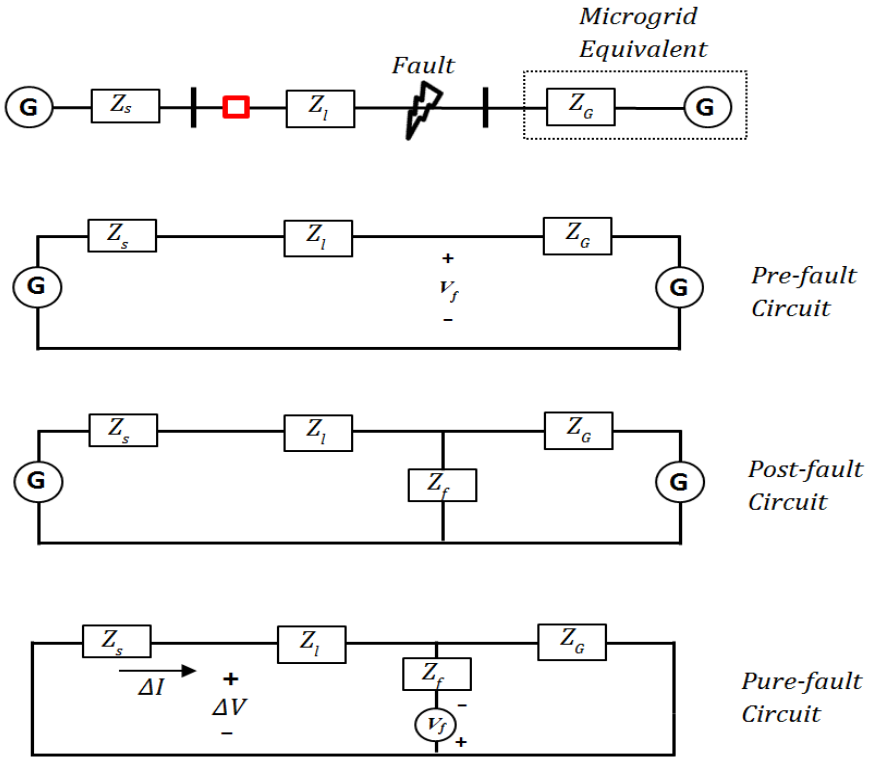

Figure 7: Example of superimposed quantities analysis

penetration. However, the trajectory of the calculated incremental impedances could depend greatly on inverter's control strategy, inverter's pre-fault operating conditions and fault location. Therefore, tuning protection elements which depend on tracking incremental impedance trajectories in high PV penetration microgrids could be very complicated or even not possible.

3 Detection of Faults in Microgrids with High PV Penetration

As discussed in section 2, current-controlled inverters limit their output current during faults based on their power reference. As a result, PV inverters fault current contribution could be less than 1 p.u based on pre-fault power output. Therefore, it is very challenging, or even not possible, to use conventional overcurrent protection schemes for protecting microgrids with high PV penetration. In this section, we discuss several inverter-based non-overcurrent fault detection schemes suitable for microgrids with significant PV penetration.

3.1 Voltage-based Protection

As discussed in section 2, PV inverters would reduce their terminal voltages to limit their current injection during faults. Thus, one of the simplest techniques to detect faults is to monitor inverter's terminal voltage. However, inverter's terminal voltage changes over the course of normal operation due to load switching, capacitors switching and other normal operation reasons. Thus, depending on the microgrid, it could be hard to design voltage-based protection that is secure and reliable for all modes of operation.

3.2 Superimposed Voltage-based Protection

For this method, faults are detected based on *voltage change* at the terminals of the inverter. This voltage change is primarily driven by the fault and thus could be used to detect faults. This is similar to the superimposed quantities-based protection presented in section 2.4.2. A simple delta filter, [19], could be used to calculate the voltage change as shown in Fig.8.

This method could provide more protection security over the basic voltage-based protection since it is immune to the slow changes of normal operation voltage. Additionally, it should be easier to adjust the protection threshold for this method as compared to the voltage-based method. Meanwhile, this method require more processing than the simple voltage-based method thus it will be more costly. Similar to the voltage-based method, capacitor switching off could cause significant enough voltage drop that could cause the protection to trip. Depending on the particular microgrid, it might be essential to add special measures to avoid erroneous tripping for capacitor switching.

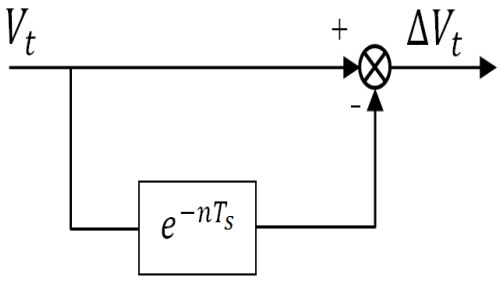

Figure 8: Delta filter used for superimposed voltage-based detection

3.3 Monitoring Terminal Negative Sequence Voltage

As discussed in section 2.2, under unbalanced faults, current-controlled inverters will, to a good extend, maintain balanced undistorted positive sequence current at the terminals of the inverter but the inverter terminal voltage will be unbalanced. In light of the sequence components equivalent circuit of a current-controlled shown in Fig.3, unbalanced faults could be detected by monitoring the negative sequence component of the inverter's terminal voltage. This method provide more security as compared to the basic voltage-based protection since negative sequence voltage would typically increase relatively significantly during unbalanced faults thus will provides good discrimination between normal operation and faults. The obvious drawback of this technique is that it will only work for unbalanced faults and will be insensitive to three phase faults.

3.4 Monitoring Zero Sequence current

Typically, PV inverters as connected to the grid through a Delta-Wye grounded transformers. As a result, during unbalanced faults, the zero sequence current on the high voltage side of the interface transformer would typically increase relatively significantly given that it is not controlled by the inverter but rather governed by the grid under fault. Therefore, monitoring zero sequence current at the high voltage side of the interface transformer could be an easy and effective method to detect faults involving ground such as single line to ground and two line to ground faults.

3.5 Impedance-based Fault Detection

As discussed in section2, low fault current contribution of inverters is mainly caused by the inverter controller actions and not because of network impedance. As a matter of fact, the impedance of the microgrid, as defined by the impedance bus matrix for instance, would change due to the presence of the fault regardless of the attributes of the electrical source. However, the presence of the fault would not result in high fault current from the current-controlled inverter, the way it typically would for a conventional source, due to the control actions of the inverter. As a result, the voltage at the terminals of the inverter would typically decrease more than it would for a conventional source. Based on that, faults could be detected based on monitoring impedance changes at the terminals of the inverter instead of current changes. During design stage, short circuit studies would be conducted to determine impedance threshold values that indicates faults at different inverters. A fault is declared whenever the impedance measured at the inverter falls below its impedance threshold value. While it is typically possible to detect occurrence of faults based on impedance drop, it is important to notice that due to the typically small sizes of microgrid feeders and feeder tapping, it is hard to use the value of the measured impedance to coordinate operation of different relays or to identify protection zones.

This method provides more security of operation to the relay as compared to the voltage-based method. However, it is more expensive since an extra protection elements, i.e. impedance element, will have to be installed at each inverter.

4 Simulation Study

In this section, detailed time-domain simulation of PV inverters is presented to highlight the behaviour of PV inverters under faults. MATLAB/SimPowerSystems was used to run all time-domain simulations. Inverter-interfaced generators are modelled as current-controlled inverters with a real/reactive-power control outer loop in the $dq-$frame. Inverters are modelled using averaged three phase voltage-source converter models as depicted in Fig.9, see [11] for modelling details.

For this simulation study, we have used the microgrid test feeder presented in [23]. Fig.10 shows a single line diagram of the test feeder. Load values were modified to obtain a reasonable power flow solution in steady state. Feeder conductors parameters were modeled based on impedance values obtained from IEEE 141-1993 [24].

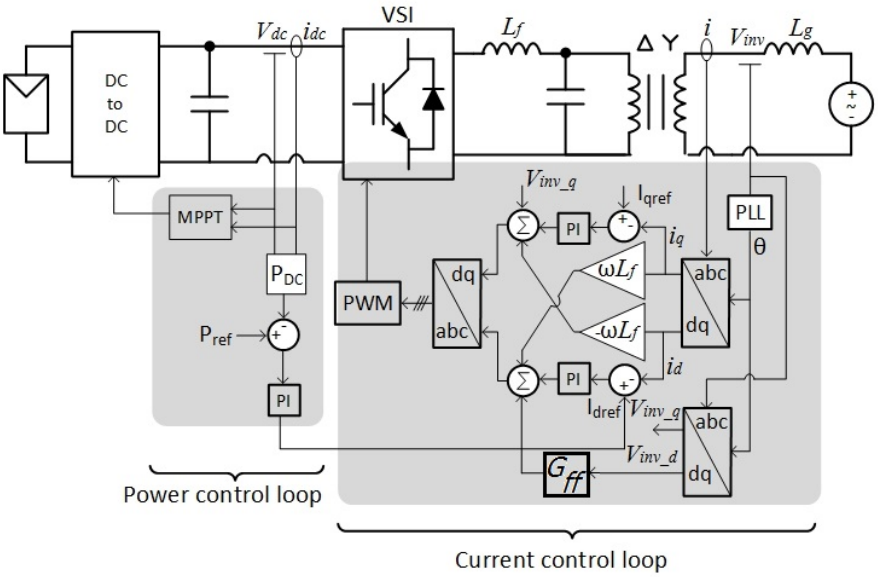

Figure 9: Inverter and controller modelling

4.1 PV inverter behavior under faults

In this section the behavior of PV inverter under faults is presented. Two faults are tested at *location* 1: a three phase fault and a single line to ground fault. Figures 11, 12, 13 and 14 shows the performance of inverter *PV1* under the three phase fault. It is clear from these results that the terminal voltage of the inverter dropped while the inverter's current injection did not increase significantly. Additionally, the output of the inverter remained balanced as expected, except for short time during initial fault transients.

Figures 15, 16, 17 and 18 show the performance of inverter *PV1* for the single line to ground fault. In this case, the current injected from the inverter remained almost balanced although a small negative sequence current did flow through the inverter. Note that as discussed in section 2.4.1, for the analysis of negative-sequence based protection elements,

the negative sequence current magnitude and angle during the fault depend on the inverter controller characteristics.

Note that for this case, currents were measured on the high voltage side of the Delta-Wye inverter's interface transformer. Therefore, the unbalance shown in Fig.16 is primarily driven by the zero sequence component shown in Fig.18 which is driven by the network.

4.2 Comparison of Fault Detection Schemes

In this section, we test the performance of the various fault detection schemes presented in section 3. Several fault locations were tested as part of this study. However, only the results for the two fault locations indicated on Fig.10 are presented in this report. For each location three faults are tested, namely three phase, single phase to ground and line to line fault. Fault testing was carried out for both grid-connected and islanded modes of operation. The results for location 1 are shown in Figures 19, 20 and 21 for grid connected mode and in Figures 22, 23 and 24 for islanded mode of operation.
Similarly, results for location 2 are shown in Figures 25, 26 and 27 for grid connected mode and in Figures 28, 29 and 30 for islanded mode of operation.

The following conclusions could be drawn based on these results:

- As mentioned in section 4.2, some of the schemes could only detect certain faults. For example, negative sequence voltage detection can only work for unbalanced faults and zero sequence current detection can only work for faults involving the ground.
- In the islanded mode of operation, and due to the size of the microgrid, the measurement of all relays are almost identical during faults. This fact makes the identification of fault location harder.
- Ultimately, design of fault detection and protection schemes for microgrids will have to depend on the particulars of the specific microgrid such as, feeder size, inverter-based resources penetration, modes of operation, and desired reliability level.

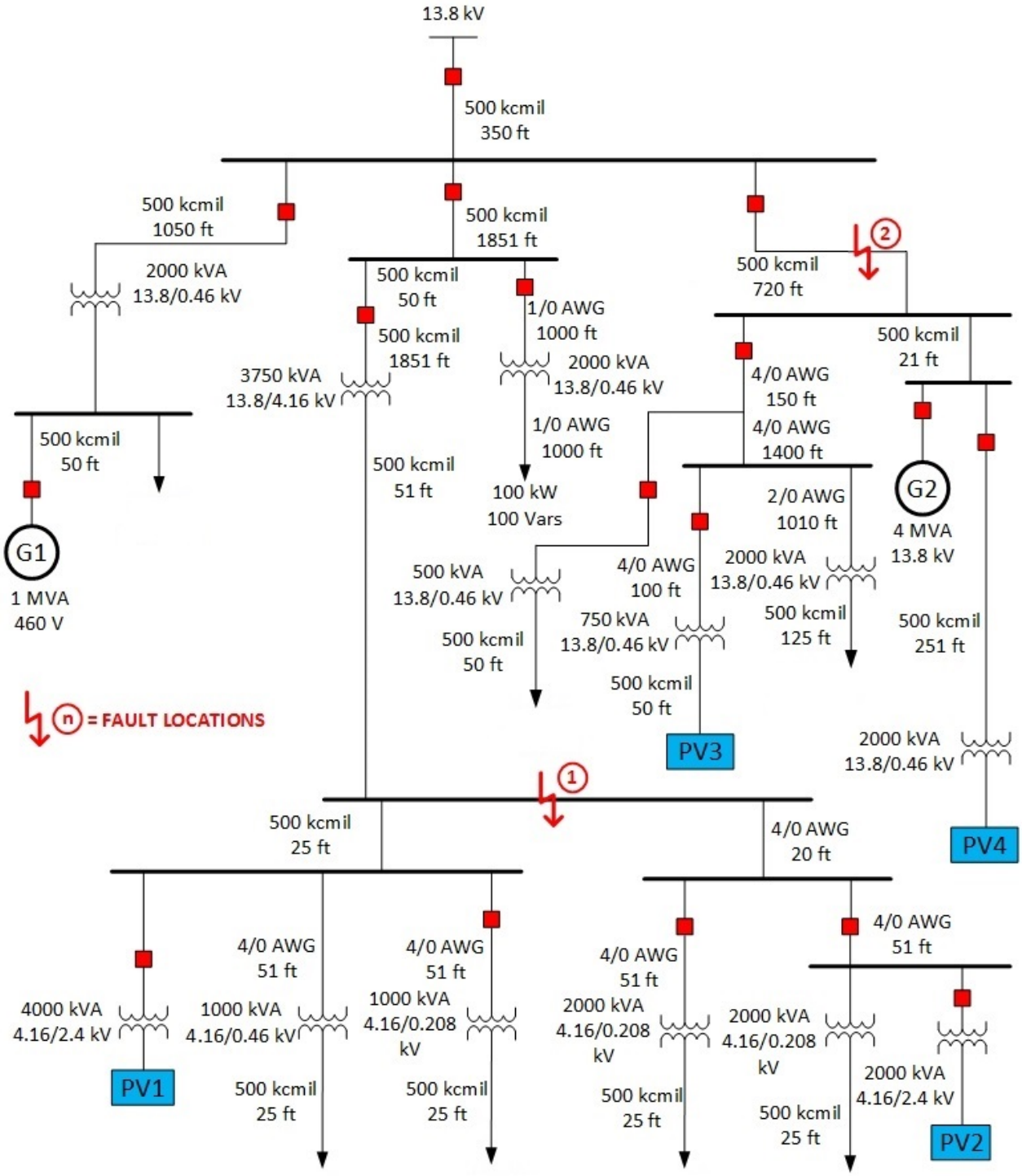

Figure 10: Microgrid used for the simulation study

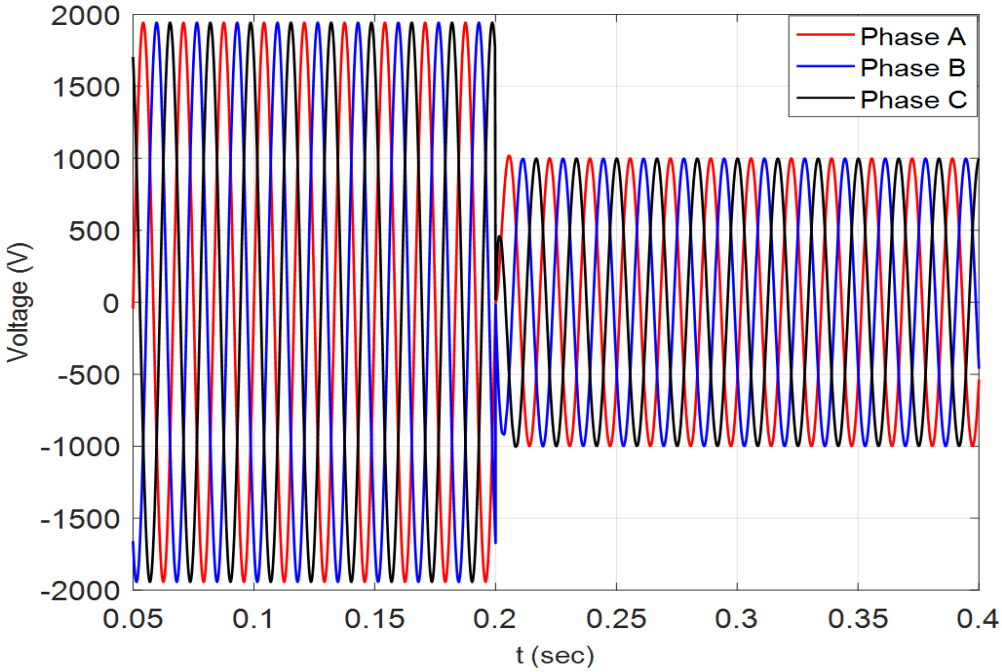

Figure 11: PV1 Inverter terminal voltage under three phase fault

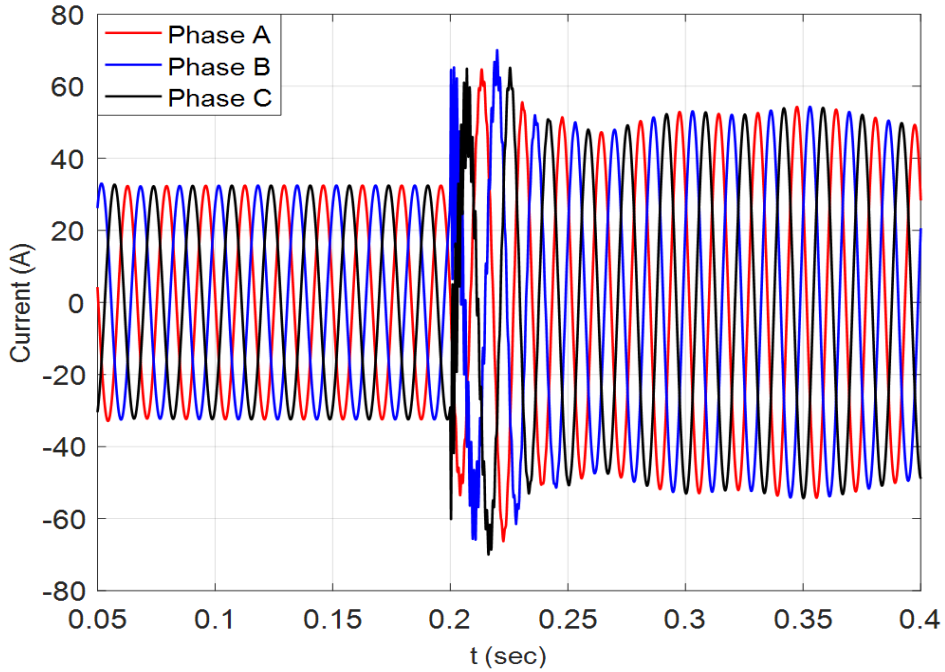

Figure 12: PV1 Inverter terminal current under three phase fault

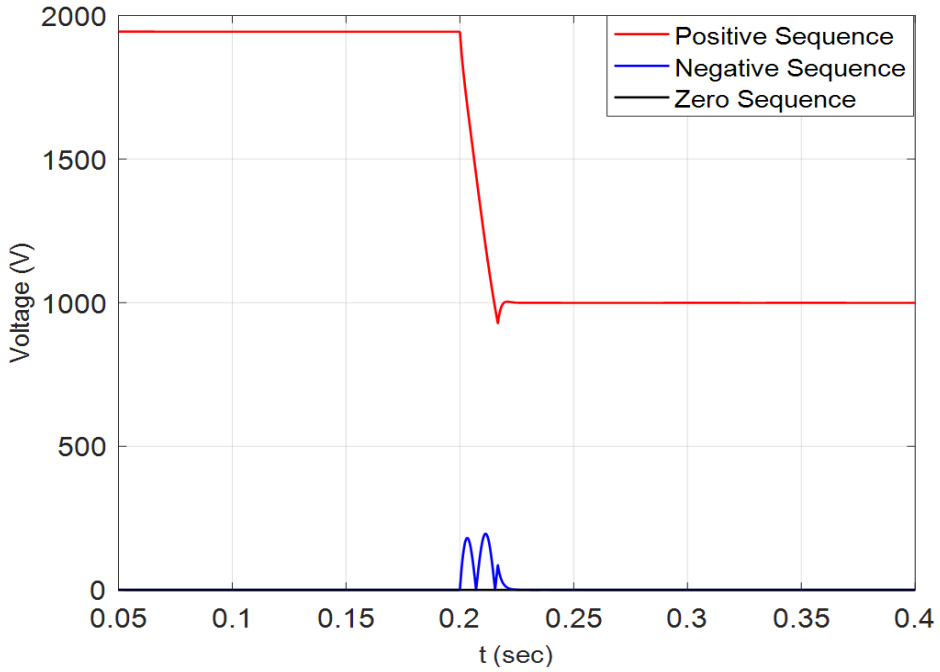

Figure 13: Sequence components of PV1 inverter terminal voltage under three phase fault

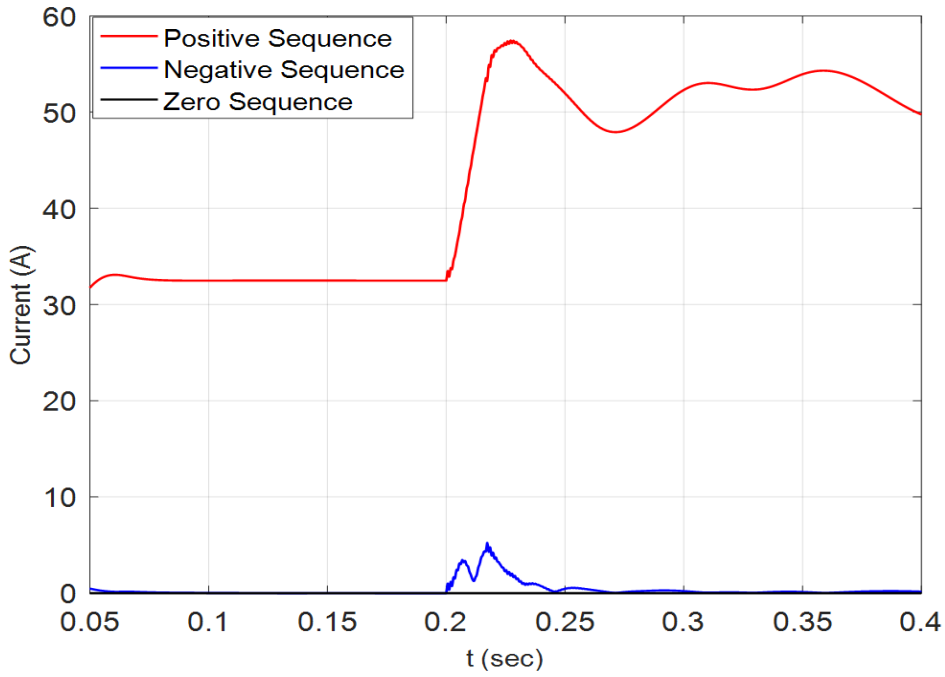

Figure 14: Sequence component of PV1 inverter terminal current under three phase fault

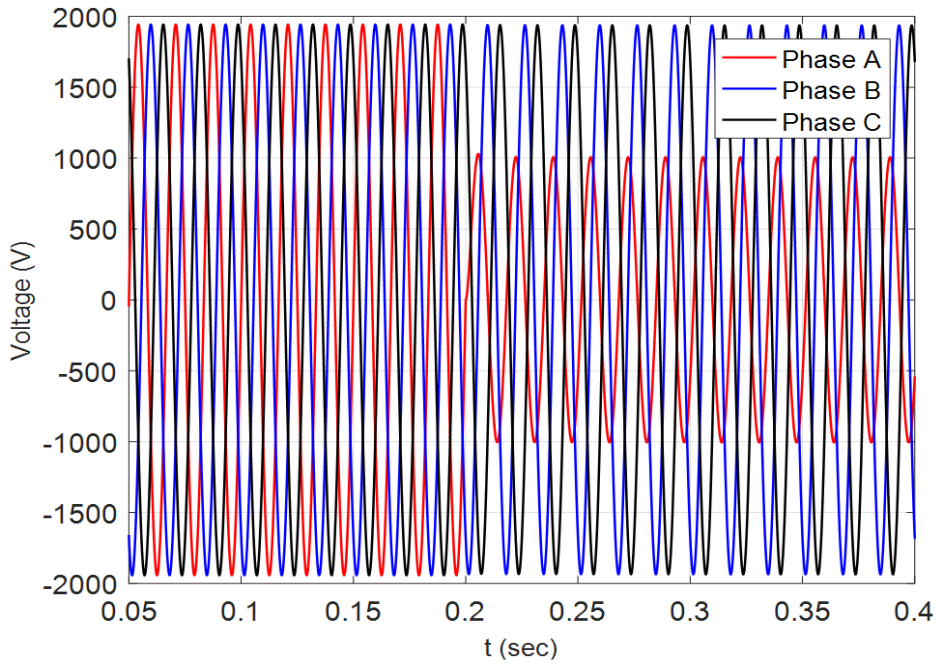

Figure 15: PV1 Inverter terminal voltage under single line to ground fault

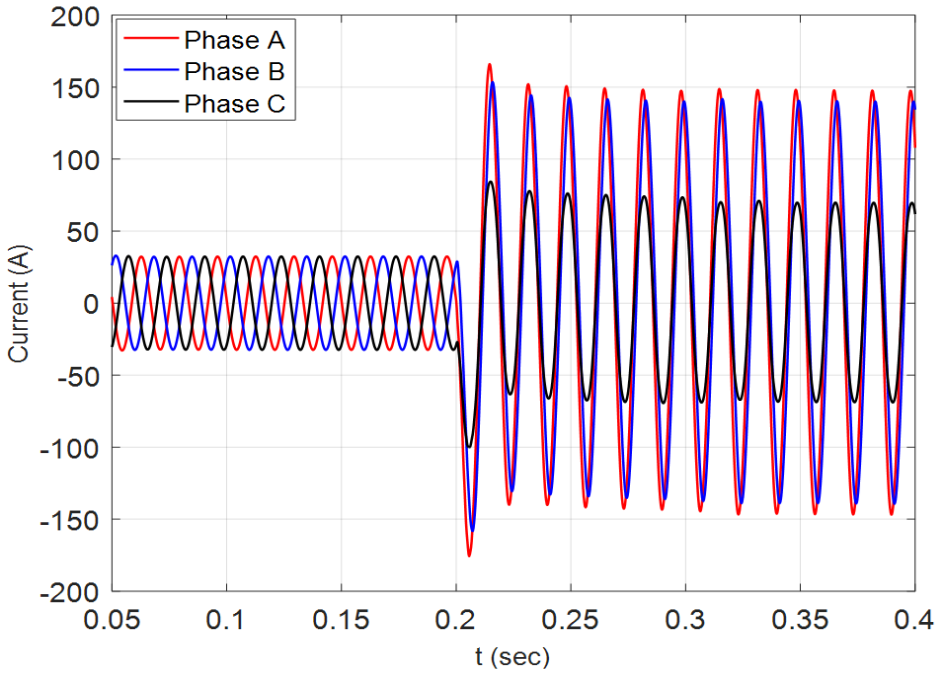

Figure 16: PV1 Inverter terminal current under single line to ground fault

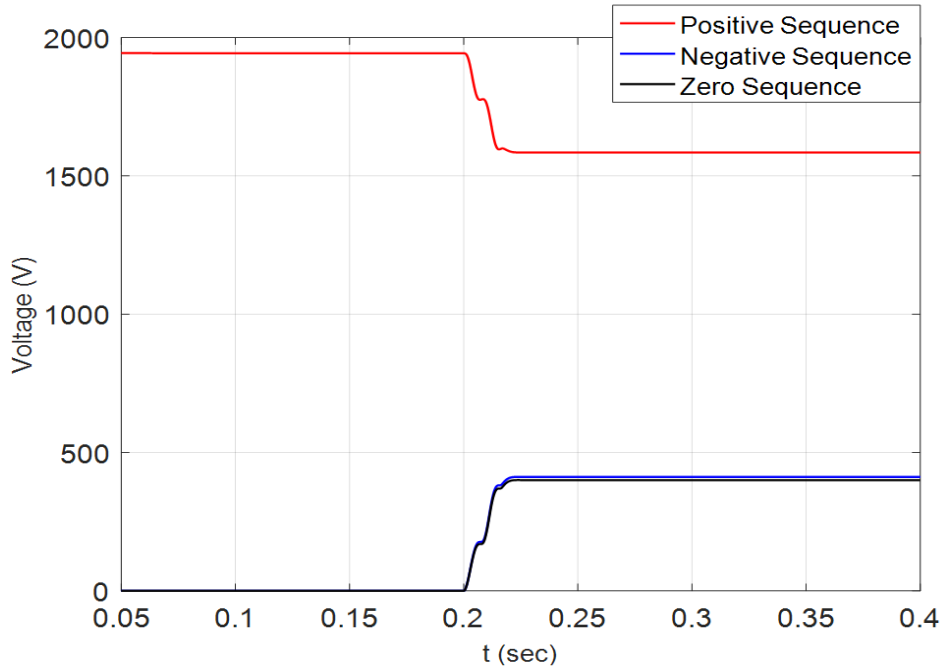

Figure 17: Sequence components of PV1 inverter terminal voltage under single line to ground fault

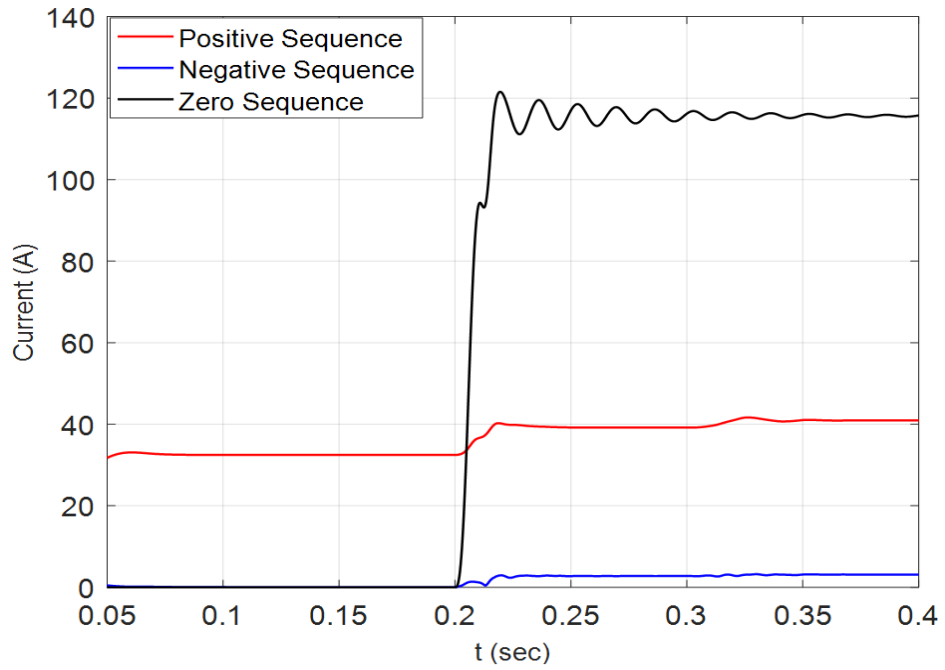

Figure 18: Sequence component of PV1 inverter terminal current under single line to ground fault

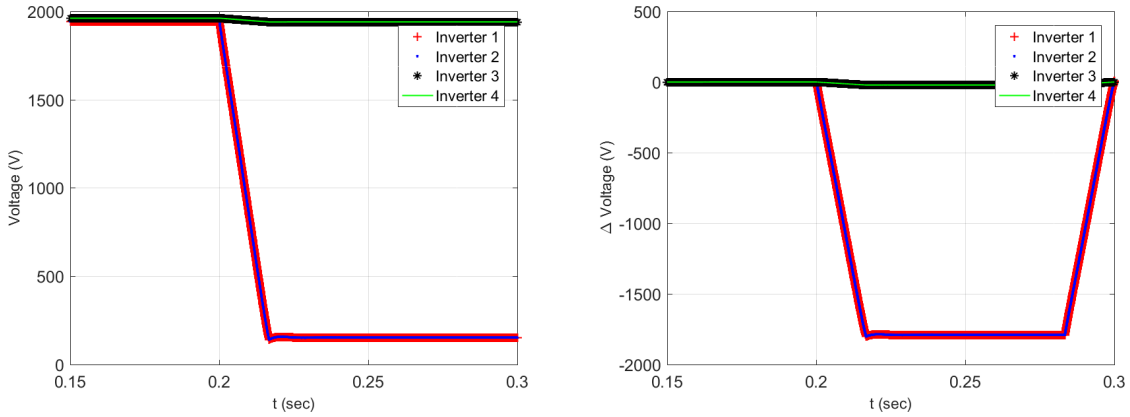

(a) (b)

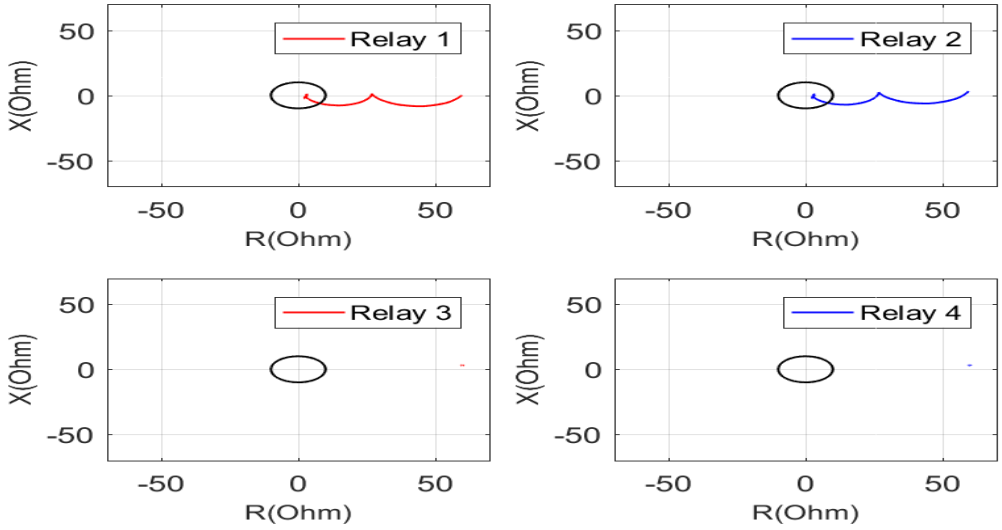

(c)

Figure 19: Relays Performance for a 3 phase fault at location 1 under grid connected mode (a) Voltage Relay (b) Superimposed Voltage Relay (c) Impedance Relay

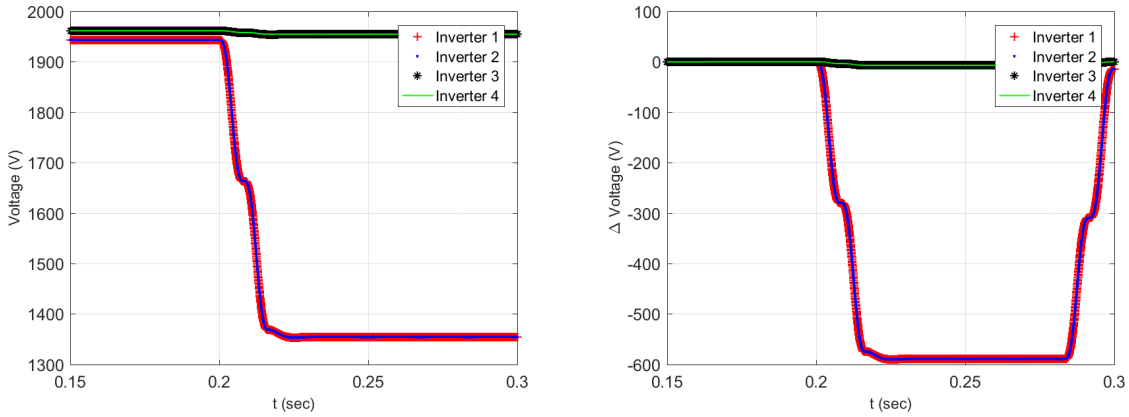

(a)

(b)

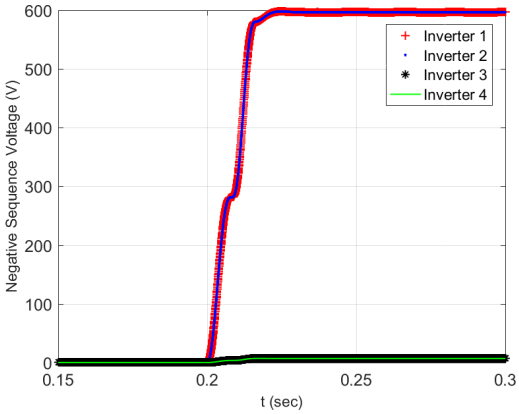

(c)

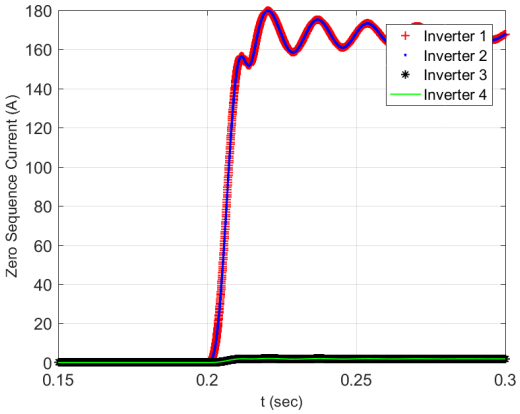

(d)

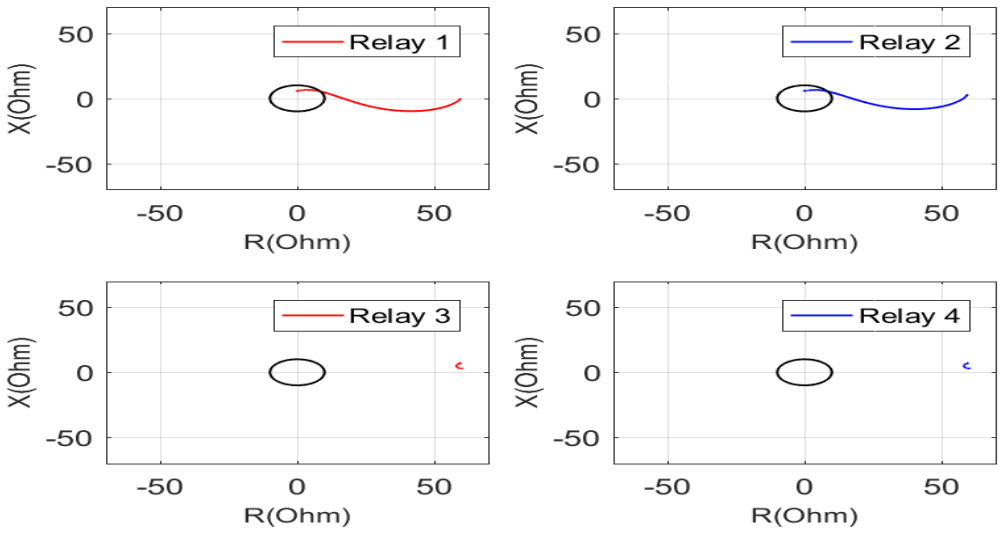

(e)

Figure 20: Relays Performance for a phase A to ground fault at location 1 under grid connected mode (a) Voltage Relay (b) Superimposed Voltage Relay (c) Negative Sequence Voltage Relay (d) Zero Sequence Current Relay (e) Impedance Relay

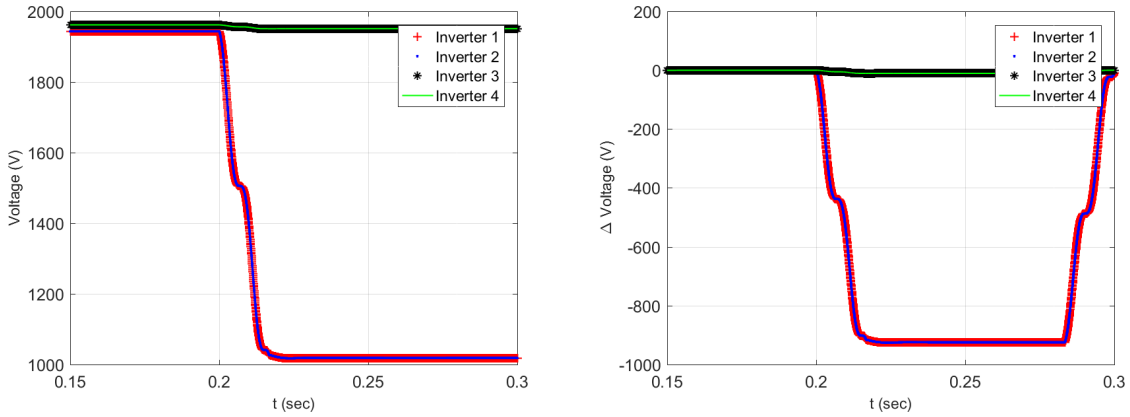

(a)

(b)

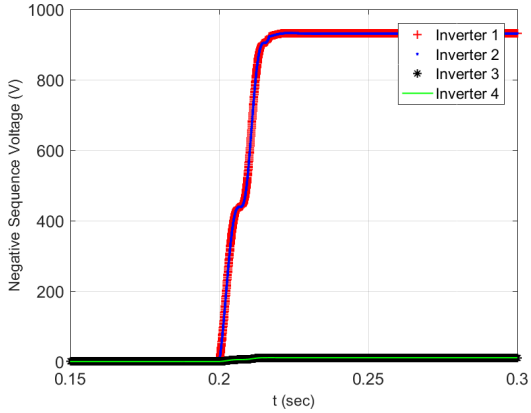

(c)

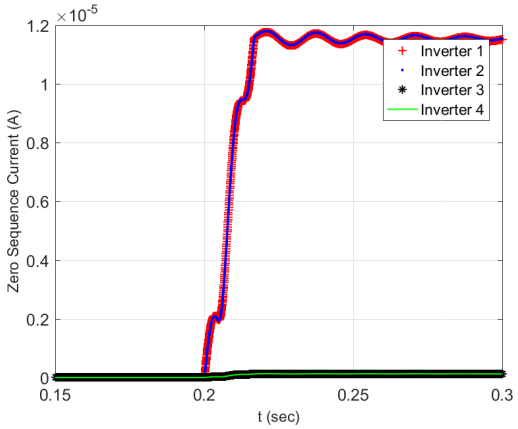

(d)

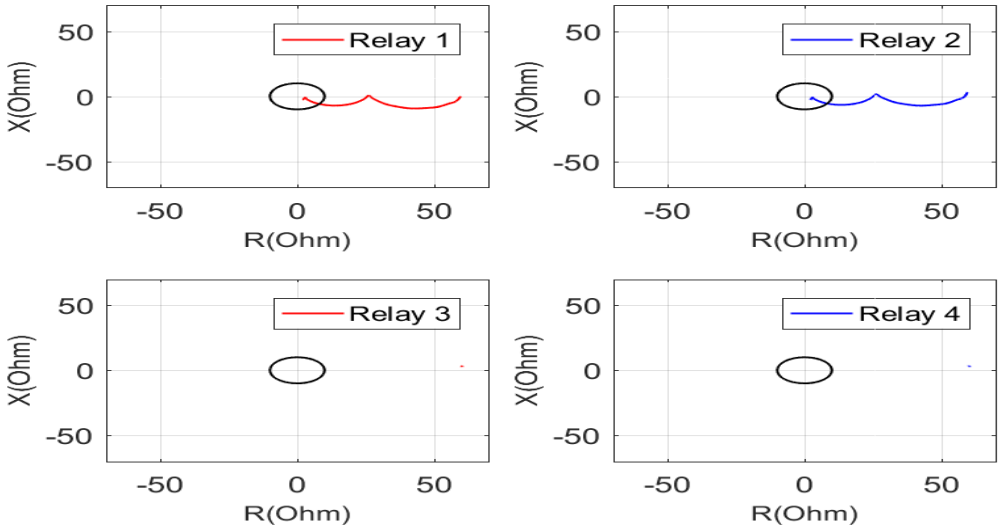

(e)

Figure 21: Relays Performance for a phase A to phase B fault at location 1 under grid connected mode (a) Voltage Relay (b) Superimposed Voltage Relay (c) Negative Sequence Voltage Relay (d) Zero Sequence Current Relay (e) Impedance Relay

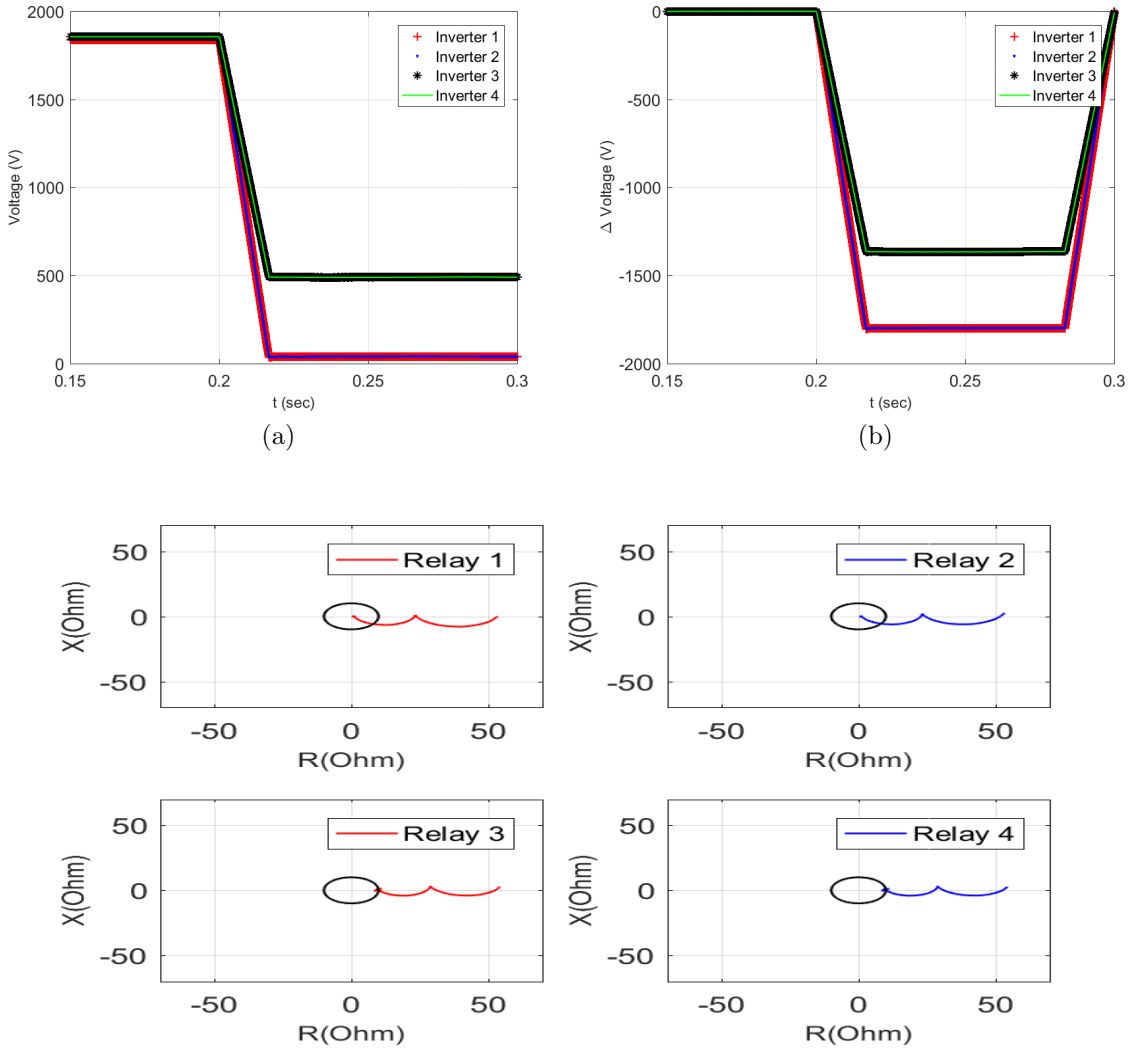

(a)

(b)

(c)

Figure 22: Relays Performance for a 3 phase fault at location 1 under islanded mode (a) Voltage Relay (b) Superimposed Voltage Relay (c) Impedance Relay

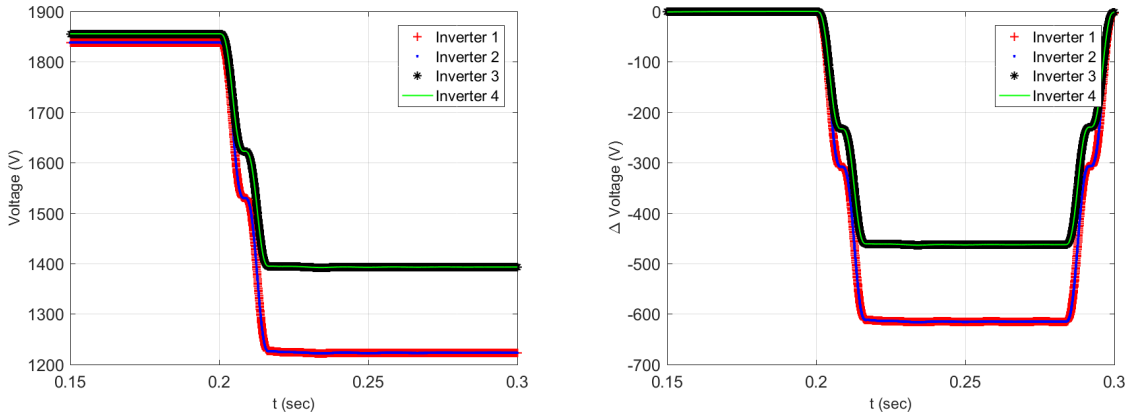

(a)

(b)

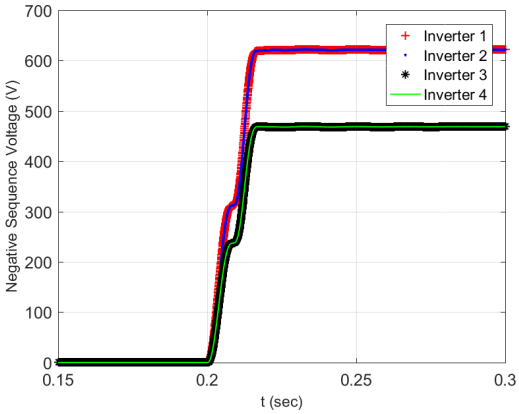

(c)

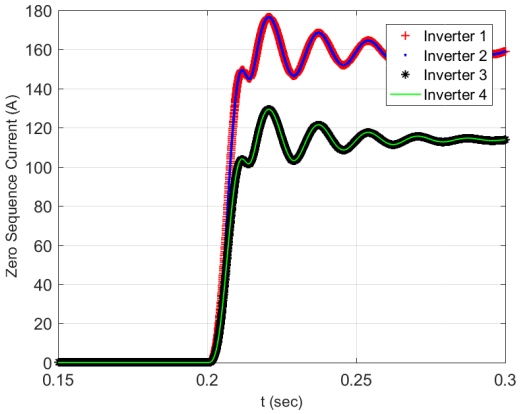

(d)

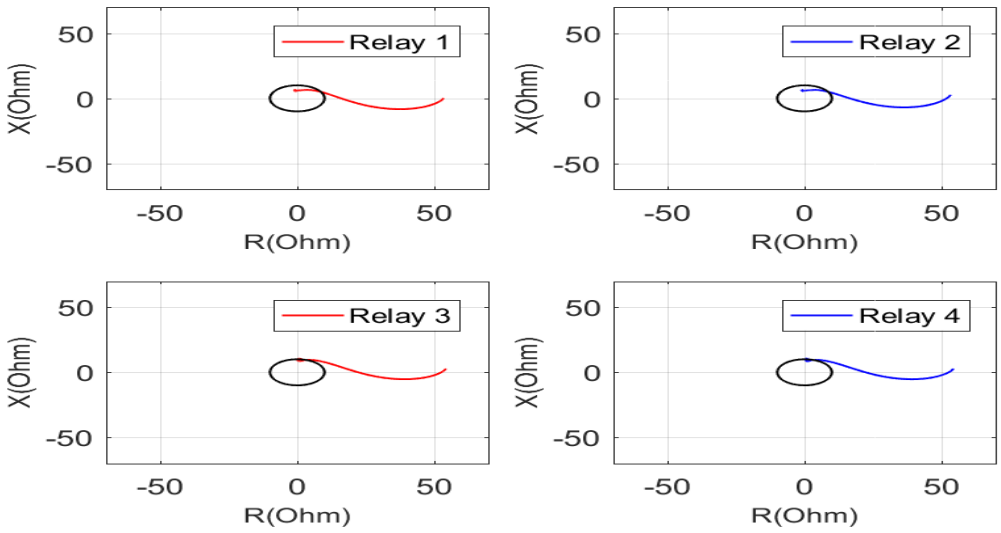

(e)

Figure 23: Relays Performance for a phase A to ground fault at location 1 under islanded mode (a) Voltage Relay (b) Superimposed Voltage Relay (c) Negative Sequence Voltage Relay (d) Zero Sequence Current Relay (e) Impedance Relay

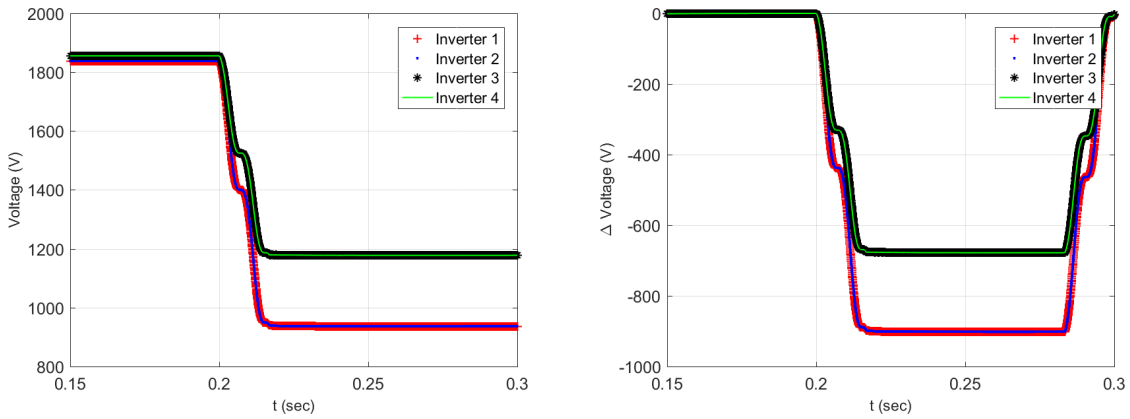

(a)

(b)

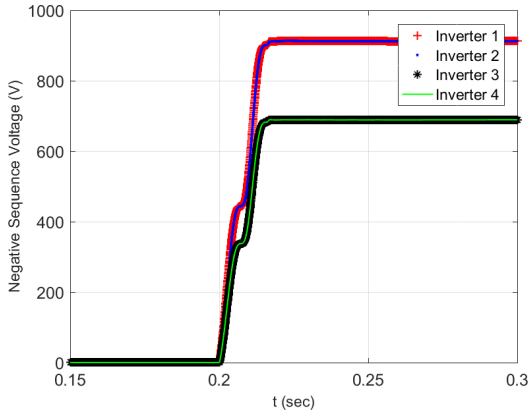

(c)

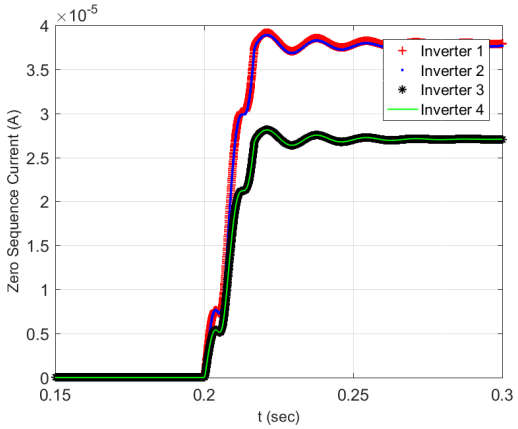

(d)

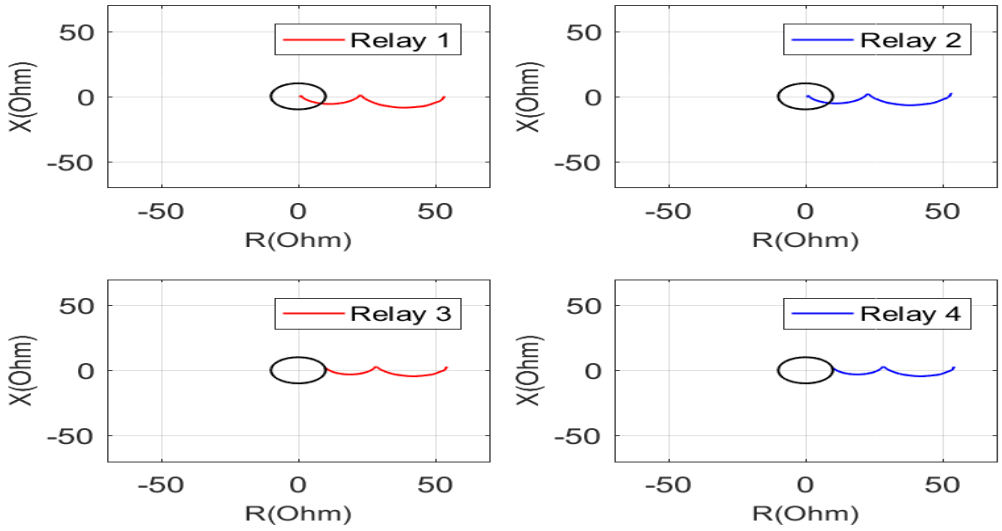

(e)

Figure 24: Relays Performance for a phase A to phase B fault at location 1 under islanded mode (a) Voltage Relay (b) Superimposed Voltage Relay (c) Negative Sequence Voltage Relay (d) Zero Sequence Current Relay (e) Impedance Relay

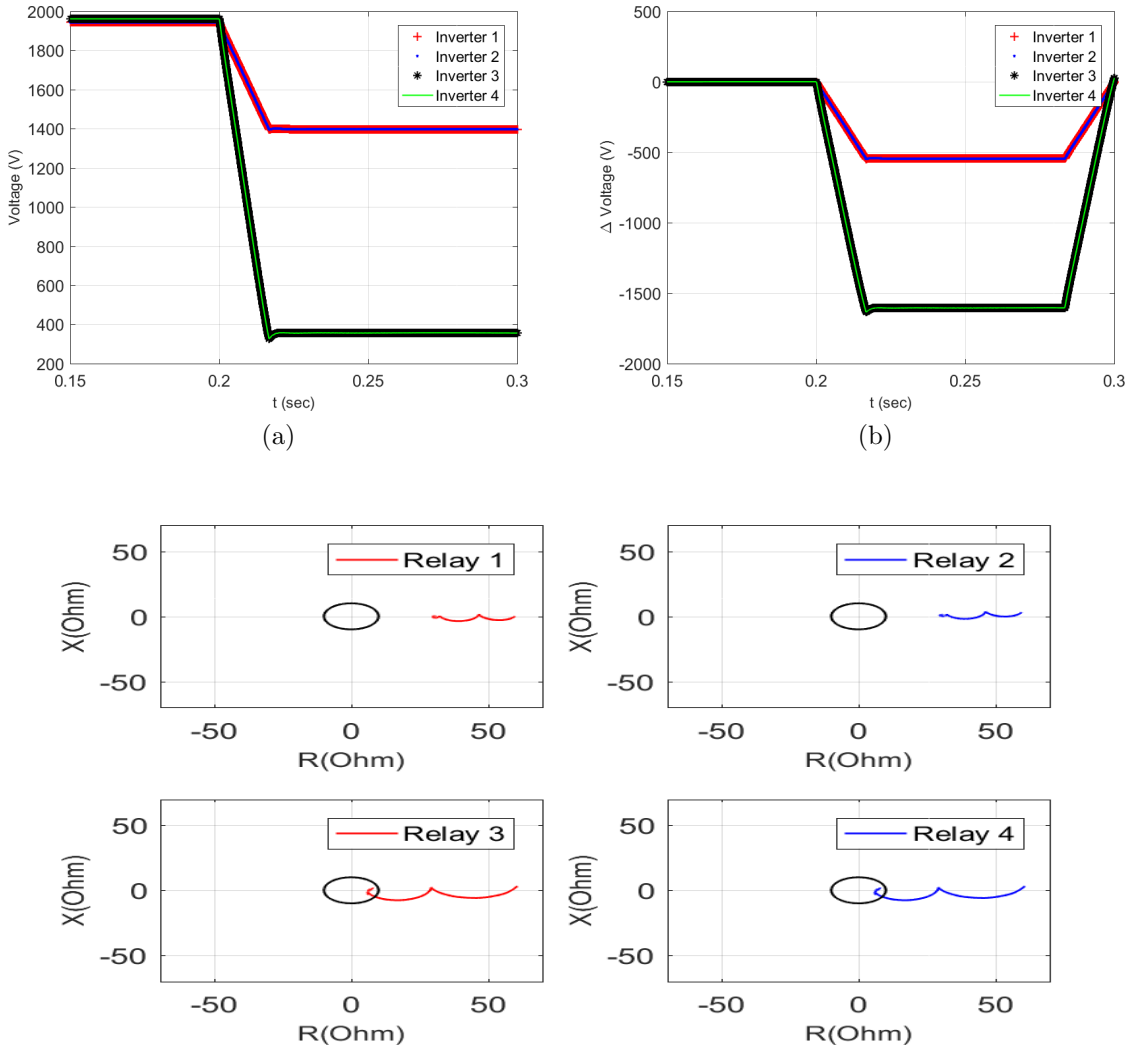

(a)

(b)

(c)

Figure 25: Relays Performance for a 3 phase fault at location 2 under grid connected mode (a) Voltage Relay (b) Superimposed Voltage Relay (c) Impedance Relay

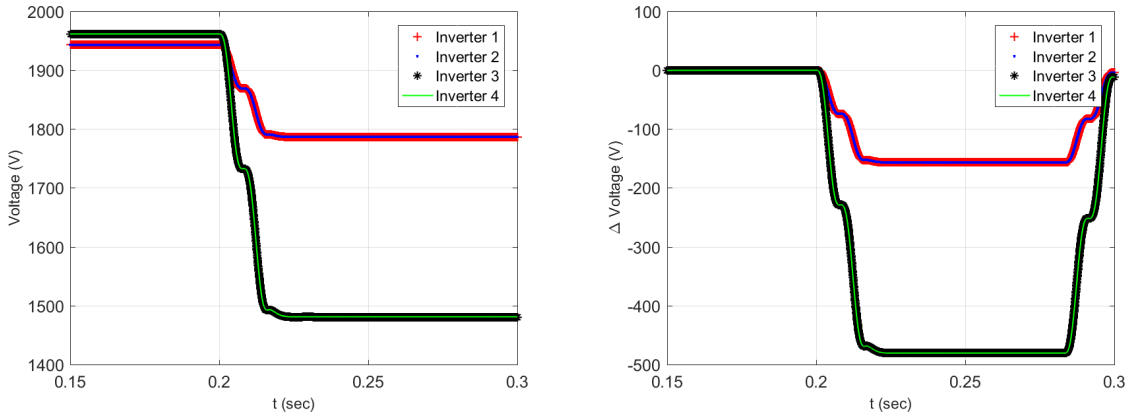

(a)

(b)

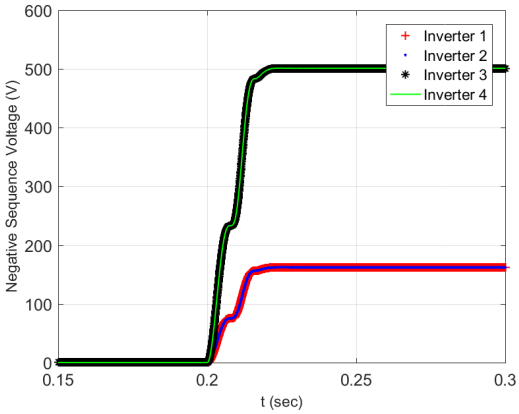

(c)

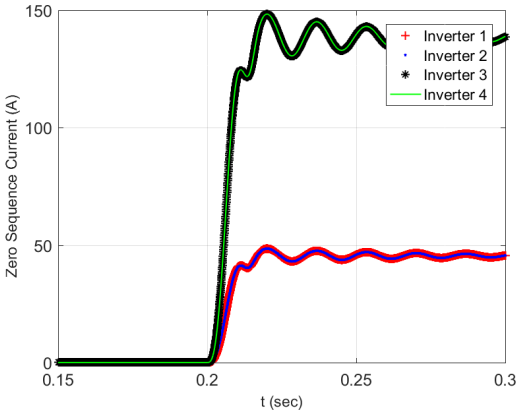

(d)

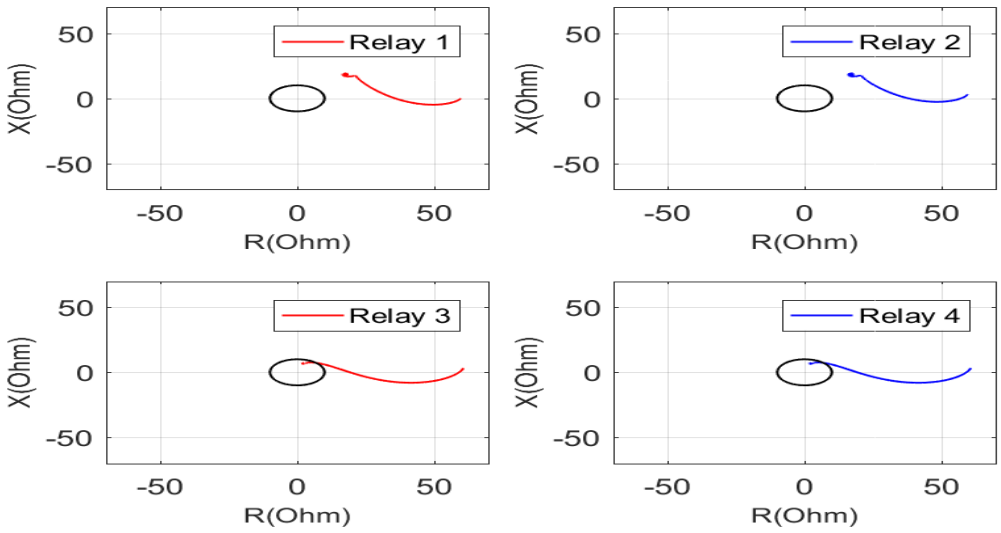

(e)

Figure 26: Relays Performance for a phase A to ground fault at location 2 under grid connected mode (a) Voltage Relay (b) Superimposed Voltage Relay (c) Negative Sequence Voltage Relay (d) Zero Sequence Current Relay (e) Impedance Relay

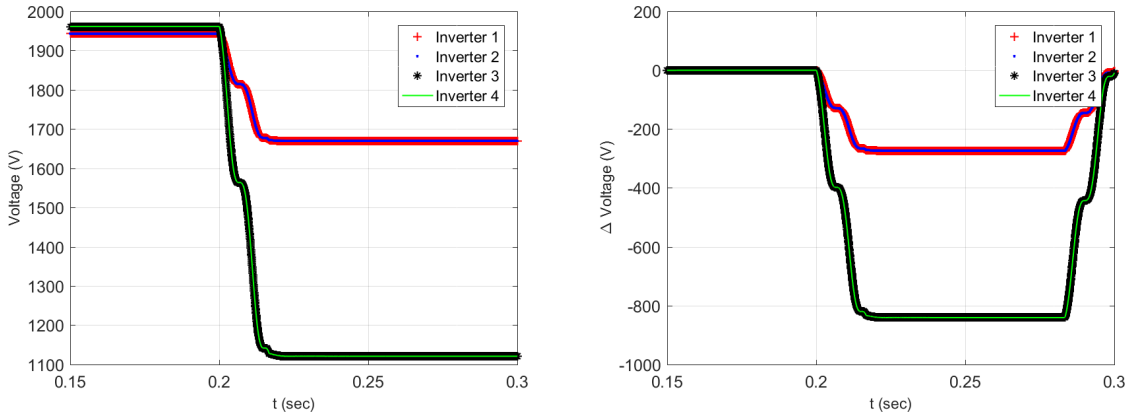

(a)

(b)

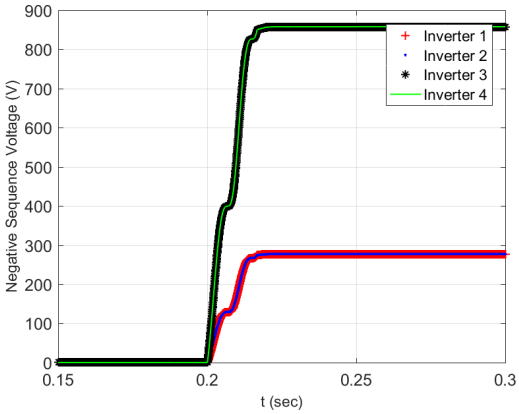

(c)

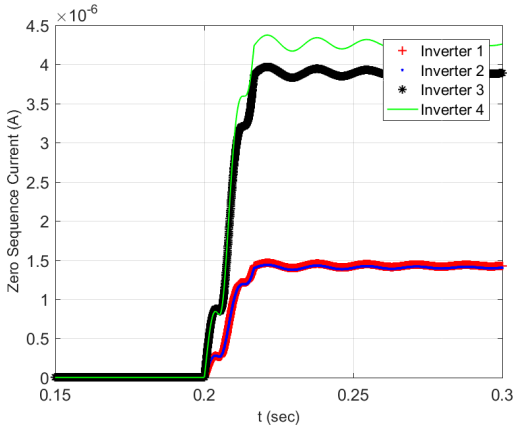

(d)

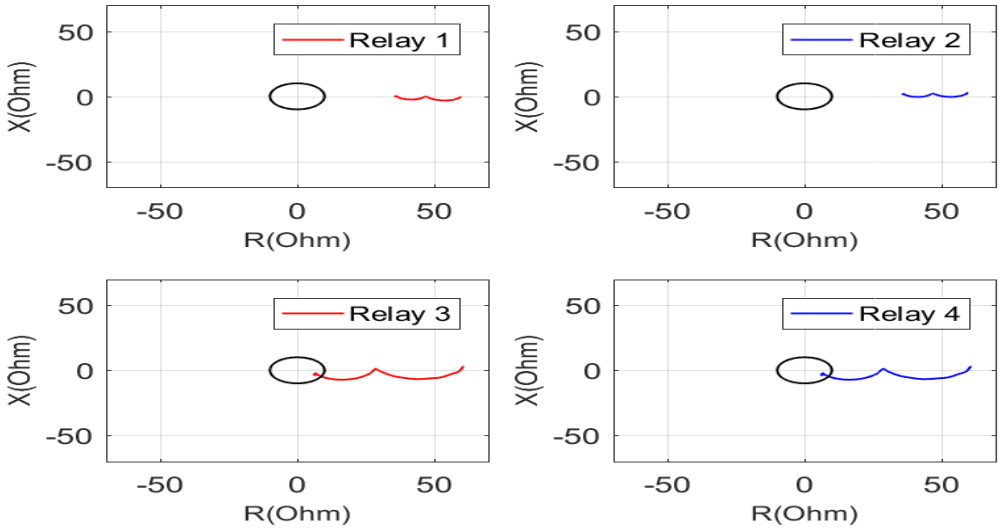

(e)

Figure 27: Relays Performance for a phase A to phase B fault at location 2 under grid connected mode (a) Voltage Relay (b) Superimposed Voltage Relay (c) Negative Sequence Voltage Relay (d) Zero Sequence Current Relay (e) Impedance Relay

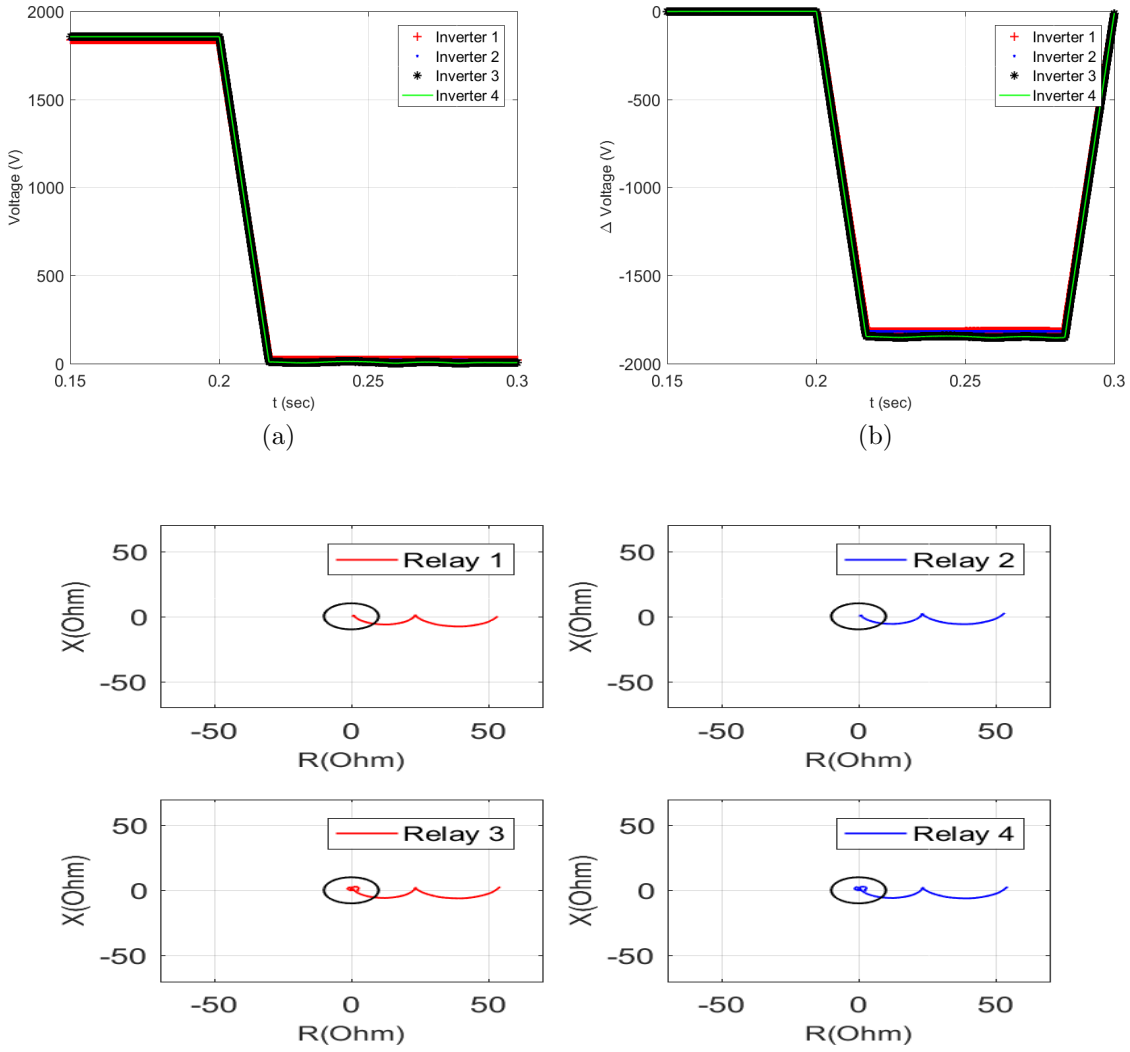

Figure 28: Relays Performance for a 3 phase fault at location 2 under islanded mode (a) Voltage Relay (b) Superimposed Voltage Relay (c) Impedance Relay

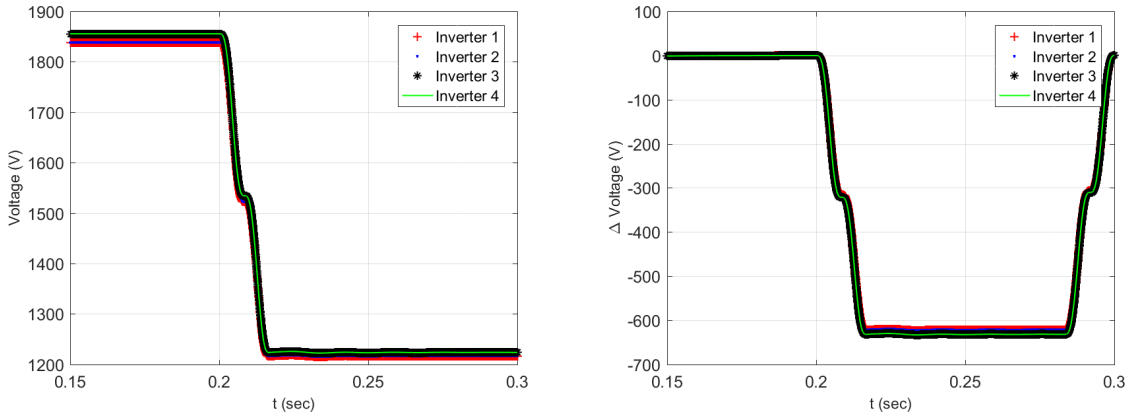

(a)

(b)

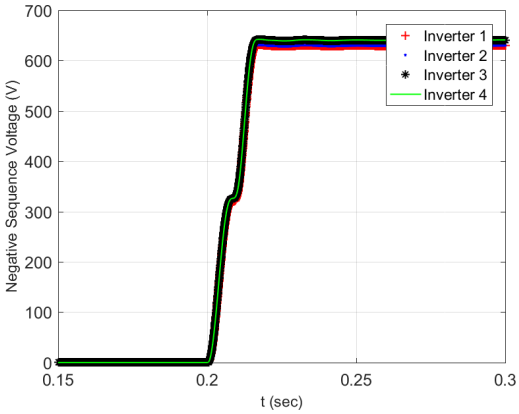

(c)

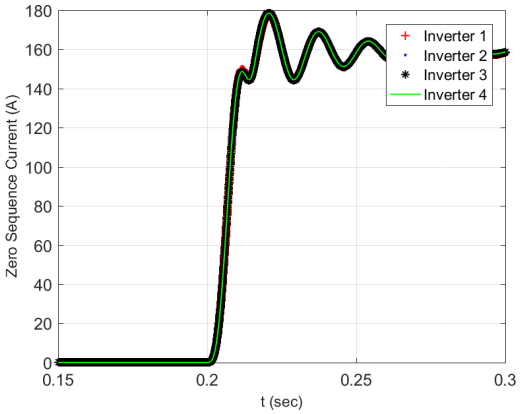

(d)

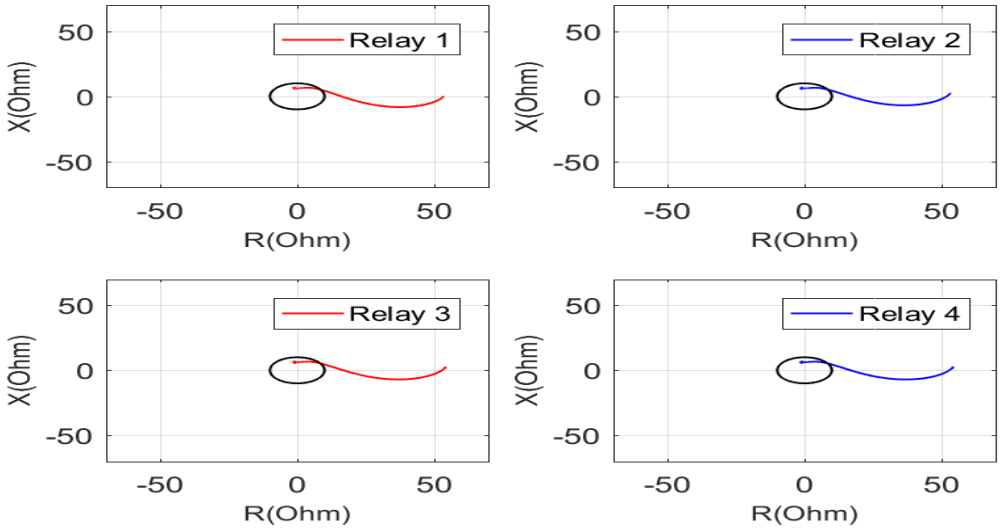

(e)

Figure 29: Relays Performance for a phase A to ground fault at location 2 under islanded mode (a) Voltage Relay (b) Superimposed Voltage Relay (c) Negative Sequence Voltage Relay (d) Zero Sequence Current Relay (e) Impedance Relay

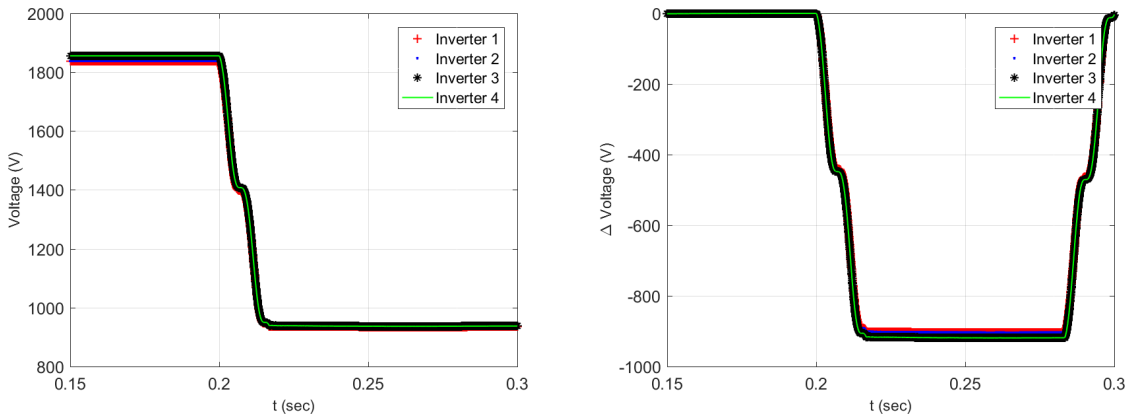

(a)

(b)

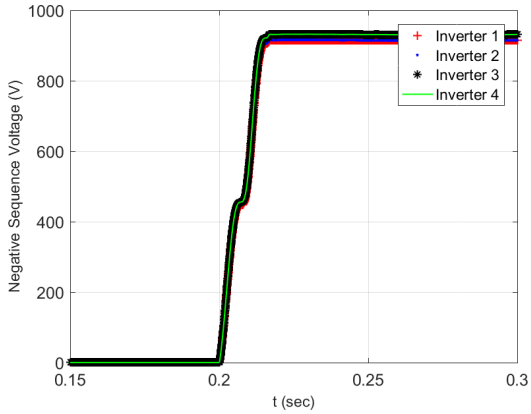

(c)

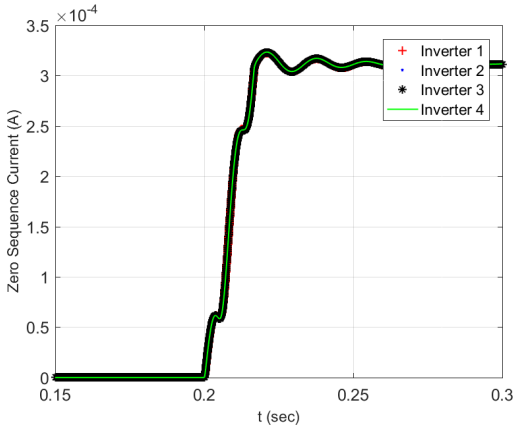

(d)

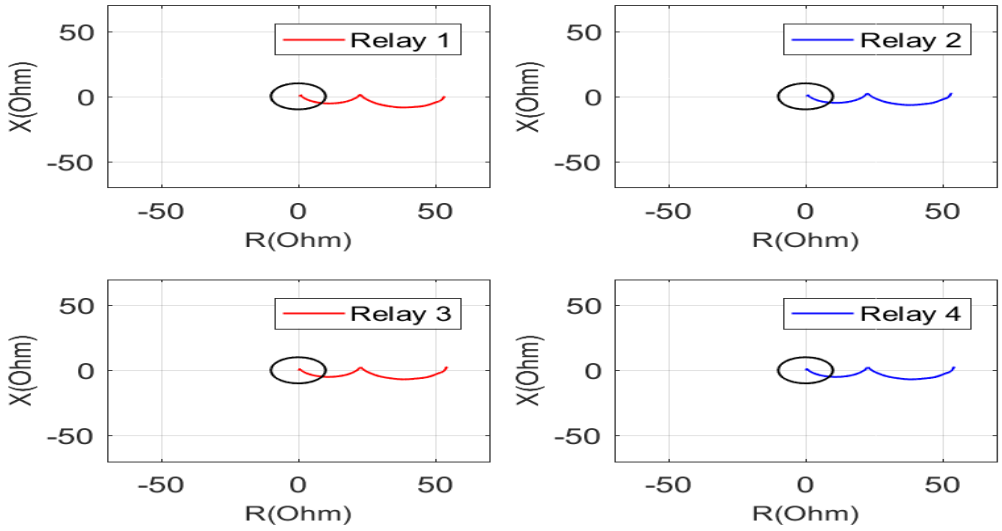

(e)

Figure 30: Relays Performance for a phase A to phase B fault at location 2 under islanded mode (a) Voltage Relay (b) Superimposed Voltage Relay (c) Negative Sequence Voltage Relay (d) Zero Sequence Current Relay (e) Impedance Relay

5 Conclusions

The overall objective of this project is to investigate the challenges facing efficient microgrid protection design and to develop protection schemes for variety of microgrid configurations including radial, mesh and dynamic topology microgrids.

In this report, analysis of PV current-controlled inverters under balanced and unbalanced faults was presented. Based on the that analysis, it was shown that a PV inverter can be represented for fault studies as a constant-power current source in the positive sequence network and as open circuit for negative and zero sequence. Additionally, the impact of PV inverters on negative sequence based directional elements and superimposed quantities-based elements was studied.

Since fault current contribution of PV inverters depends on pre-fault power output of the PV and the location of the fault, the short circuit current of the inverter could be less than 1 pu based. Thus, using overcurrent protection to detect faults in microgrids with high penetration might not be possible. Several non-overcurrent fault detection schemes are discussed in this report for microgrids with high PV penetration. A detailed time-domain simulation study is presented to assess the performance of the presented fault detection schemes under different microgrid modes of operation.

Future work will focus on conducting hardware-in-the-loop testing of PV inverters to validate different fault detection schemes and to test the impedance-based protection scheme proposed in [10]. Additionally, determining fault location once the fault is detected remains a challenge for microgrids with high penetration of inverters. Several methods will be investigated to determine fault location including the use of micro-PMUs data and communication-assisted methods.

References

[1] H. Al-Nasseri, M. A. Redfern, and F. Li, "A voltage based protection for micro-grids containing power electronic converters," in *2006 IEEE Power Engineering Society General Meeting*, pp. 7 pp.–, 2006.

[2] M. Zamani, T. Sidhu, and A. Yazdani, "A protection strategy and microprocessor-based relay for low-voltage microgrids," *Power Delivery, IEEE Transactions on*, vol. 26, pp. 1873–1883, July 2011.

[3] M. A. Zamani, A. Yazdani, and T. S. Sidhu, "A communication-assisted protection strategy for inverter-based medium-voltage microgrids," *IEEE Transactions on Smart Grid*, vol. 3, pp. 2088–2099, Dec 2012.

[4] E. Sortomme, S. S. Venkata, and J. Mitra, "Microgrid protection using communication-assisted digital relays," *IEEE Transactions on Power Delivery*, vol. 25, no. 4, pp. 2789–2796, 2010.

[5] E. Casagrande, W. L. Woon, H. H. Zeineldin, and D. Svetinovic, "A differential sequence component protection scheme for microgrids with inverter-based distributed generators," *IEEE Transactions on Smart Grid*, vol. 5, pp. 29–37, Jan 2014.

[6] M. Dewadasa, A. Ghosh, G. Ledwich, and M. Wishart, "Fault isolation in distributed generation connected distribution networks," *IET Generation, Transmission Distribution*, vol. 5, pp. 1053–1061, October 2011.

[7] X. Li, A. Dyśko, and G. M. Burt, "Traveling wave-based protection scheme for inverter-dominated microgrid using mathematical morphology," *IEEE Transactions on Smart Grid*, vol. 5, pp. 2211–2218, Sept 2014.

[8] S. Saleh and R. Ahshan, "Digital multi-relay protection for micro-grid systems," in *Industry Applications Society Annual Meeting (IAS), 2012 IEEE*, pp. 1–8, Oct 2012.

[9] S. Saleh, "Signature-coordinated digital multirelay protection for microgrid systems," *Power Electronics, IEEE Transactions on*, vol. 29, pp. 4614–4623, Sept 2014.

[10] M. Elkhatib and A. Ellis, "Communication-assisted impedance-based microgrid protection scheme," in *Power and Energy Society General Meeting, 2017 IEEE*, 2017.

[11] A. Yazdani and R. Iravani, *Voltage-sourced converters in power systems: modeling, control, and applications*. John Wiley & Sons, 2010.

[12] W. M. Guo, L. H. Mu, and X. Zhang, "Fault models of inverter-interfaced distributed generators within a low-voltage microgrid," *IEEE Transactions on Power Delivery*, vol. 32, pp. 453–461, Feb 2017.

[13] A. Camacho, M. Castilla, J. Miret, J. C. Vasquez, and E. Alarcon-Gallo, "Flexible voltage support control for three-phase distributed generation inverters under grid fault," *IEEE Transactions on Industrial Electronics*, vol. 60, pp. 1429–1441, April 2013.

[14] A. Camacho, M. Castilla, J. Miret, A. Borrell, and L. G. de Vicuña, "Active and reactive power strategies with peak current limitation for distributed generation inverters during unbalanced grid faults," *IEEE Transactions on Industrial Electronics*, vol. 62, pp. 1515–1525, March 2015.

[15] F. Wang, J. L. Duarte, and M. A. M. Hendrix, "Design and analysis of active power control strategies for distributed generation inverters under unbalanced grid faults," *IET Generation, Transmission Distribution*, vol. 4, pp. 905–916, August 2010.

[16] P. Rodriguez, A. V. Timbus, R. Teodorescu, M. Liserre, and F. Blaabjerg, "Flexible active power control of distributed power generation systems during grid faults," *IEEE Transactions on Industrial Electronics*, vol. 54, pp. 2583–2592, Oct 2007.

[17] J. A. Suul, A. Luna, P. Rodríguez, and T. Undeland, "Virtual-flux-based voltage-sensorless power control for unbalanced grid conditions," *IEEE Transactions on Power Electronics*, vol. 27, pp. 4071–4087, Sept 2012.

[18] B. Fleming, "Negative-sequence impedance directional element," *Schweitzer Engineering Laboratories Inc.*, 1998.

[19] G. Benmouyal and J.Roberts, "Superimposed quantities: Their true nature and applications in relays," *Schweitzer Engineering Laboratories Inc.*, 1999.

[20] P. G. McLaren, G. W. Swift, Z. Zhang, E. Dirks, R. P. Jayasinghe, and I. Fernando, "A new directional element for numerical distance relays," *IEEE Transactions on Power Delivery*, vol. 10, pp. 666–675, Apr 1995.

[21] Z. Li, X. Lin, H. Weng, and Z. Bo, "Efforts on improving the performance of superimposed-based distance protection," *IEEE Transactions on Power Delivery*, vol. 27, pp. 186–194, Jan 2012.

[22] P. Jafarian and M. Sanaye-Pasand, "High-speed superimposed-based protection of series-compensated transmission lines," *IET Generation, Transmission Distribution*, vol. 5, pp. 1290–1300, December 2011.

[23] R. O. Salcedo, J. K. Nowocin, C. L. Smith, R. P. Rekha, E. G. Corbett, E. R. Limpaecher, and J. M. LaPenta, "Development of a Real-Time Hardwarein-the-Loop Power Systems Simulation Platform to Evaluate Commercial Microgrid Controllers," tech. rep., Massachusetts Institute of Technology, February 2016.

[24] *IEEE Standard for Recommended Practice for Electric Power Distribution for Industrial Plants*, IEEE Standard 141-1993.

DISTRIBUTION:

1 Dan Ton, Department of Energy

1 MS 1133 Abraham Ellis , 6112
1 MS 0899 Technical Library, 9536 (electronic copy)

Sandia National Laboratories